

Supplemental Material

Supplemental Method:

Immunoblotting. Equal amounts of cardiac proteins (40 µg) were heated with Laemmli loading buffer with 100 mM dithiothreitol at 70 °C for 10 min. The proteins were separated using sodium dodecyl-sulfate polyacrylamide gel electrophoresis on 9879a Bio-Rad Mini-Protean 10–200 kDa Tris-glycine gel, and then transferred onto a polyvinylidene difluoride membrane (Bio-Rad TransBlot Turbo). Protein loading and transfer was verified with Ponceau S stain. The blots were blocked in the blocking buffer (5% bovine serum albumin, 0.005% sodium azide, in 1× Tris-buffered saline/ Tween 20 (TBST) (Cell Signaling)), reacted with primary antibodies at 4 °C overnight, washed with 1× TBST, reacted with secondary antibodies at ambient temperature for 1 hr, washed with 16× TBST, then detected by chemiluminescence. All antibodies were purchased from Cell Signaling, including rabbit monoclonal IgG against GAPDH (#5174), HK1 (#2024), HK2 (#2867), ANXA2 (#8235), VIM (#5741), TGM2 (#3557), PGAM1 (#12098), LDHA/C (#3558), ALDOA (#8060), PKM1/2 (#3190), PDH (#3205); and rabbit polyclonal antibodies against ANXA5 (#8555), MSN (#3146), ATP1A1 (#3010). Primary antibodies were diluted in 1:1000 in the blocking buffer. Secondary antibodies were 1:3000 goat anti-rabbit IgG conjugated to horseradish peroxidase (#7074) in the blocking buffer.

Gas chromatography. To quantify ²H₂O enrichment levels, mouse and human plasma samples were used directly for gas chromatography MS analyses. For each sample, 20 µL of plasma was mixed with 2 µL of 10 N NaOH and 4 µL of 5% (v/v) acetone in acetonitrile. The standard curves were created by adding 0% to 20% molar ratio of ²H₂O at 11 regular intervals in 1× PBS in place of the plasma sample to the acetone. The sample mixtures were incubated at ambient temperature overnight. Acetone was extracted by adding 500 µL of chloroform and 0.5 g of anhydrous sodium sulfate. One µL of the extracted solution was analyzed on a gas chromatography mass spectrometer (Agilent 6890/5975) with a J&W DB17-MS capillary column (Agilent, 30 m × 0.25 mm × 0.25 µm) at the UCLA Molecular Instrumentation Center. The column temperature gradient was as follows: 60 °C initial, 20 °C·min⁻¹ increase to 100 °C, 50 °C·min⁻¹ increase to 220 °C, 1 min hold. The mass spectrometer operated in the electron impact mode (70 eV) and selective ion monitoring at m/z 58 and 59 with 10 ms dwell time.

Protein sample preparation. The human whole blood sample was collected in lithium heparin tubes and separated into plasma and blood cells by centrifugation (800 g, 4 °C, 5 min). Erythrocytes were isolated by centrifugation on 1:1 Histopaque-1077 (400 g, 4 °C, 30 min) followed by washing twice with PBS. Plasma samples (7 μ L; approximately 500 μ g proteins) were depleted of the 14 top abundance proteins using an Agilent Hu14 Multiple Affinity Removal System column.

Mouse hearts were excised and homogenized by a 7-mL Dounce homogenizer (Pyrex) (20 strokes) in an extraction buffer (250 mM sucrose, 10 mM HEPES, 10 mM Tris, 1 mM EGTA, 10 mM dithiothreitol, protease and phosphatase inhibitors (Pierce Halt), pH 7.4) at 4 °C, then centrifuged (800 g, 4 °C, 7 min). The pellet was collected as the total debris fraction. The supernatant was centrifuged (4,000 g, 4 °C, 30 min) and collected as the organelle-depleted cytosolic fraction. The pellet was washed, then overlaid on a 19%/30%/60% discrete Percoll gradient, and sedimented by ultracentrifugation (12,000 g, 4 °C, 10 min). Purified mitochondria were collected from the 30%/60% interface layer and washed twice. Protein concentrations were measured by bicinchoninic acid assays (Thermo Pierce).

Mouse plasma, heart, and human erythrocyte protein samples were separately digested in-solution; 200 μ g proteins were heated at 80 °C with 0.2% (w/v) Rapigest (Waters) for 5 min, then heated at 70 °C with 3 mM dithiothreitol for 5 min, followed by alkylation with 9 mM iodoacetamide in the dark at ambient temperature. Proteins were digested with 50:1 sequencing grade trypsin (Promega) for 16 h at 37 °C, then acidified with 1% trifluoroacetic acid (Thermo Pierce). Depleted human plasma samples were digested on-filter using 10,000 Da polyethersulfone filters (Nanosep; Pall Life Sciences) (1). Sample buffer was exchanged on-filter with 100 mM ammonium bicarbonate. The samples were then heated at 70 °C with 3 mM dithiothreitol for 5 min, followed by alkylation with 9 mM iodoacetamide in the dark at ambient temperature. Proteins were digested with 50:1 sequencing grade trypsin (Promega) on-filter for 16 h at 37 °C.

Two-dimensional liquid chromatography peptide separation. High-performance liquid chromatography-grade water (J.T.Baker) was used for all analytical solvent preparations. First-dimension (high-pH) separation for mouse (heart cytosol and mitochondria, plasma) and human (subject 4 and 6) samples was conducted on a Phenomenex C18 column (Jupiter Proteo C12, 4 μ m particle, 90 Å pore, 100 mm \times 1 mm dimension) at high pH using a Finnigan Surveyor liquid chromatography system. The solvent gradient was as follows: 0-2 min, 0-5% B; 3-32 min, 5-35% B; 32-37min, 80% B; 50 μ L \cdot min⁻¹; A: 20 mM ammonium formate, pH 10; B: 20 mM ammonium formate, 90% acetonitrile, pH 10. Fifty μ g of

proteolytic peptides were injected with a syringe into a manual 6-port/2-position switch valve. Twelve fractions from 16–40 min were collected, lyophilized and re-dissolved in 20 μL 0.5% formic acid with 2% acetonitrile prior to low-pH reversed-phase separation.

On-line second-dimension (low-pH) reversed-phase chromatography was performed on all samples using an Easy-nLC 1000 nano-UPLC system (Thermo Scientific) on an EasySpray C18 column (PepMap, 3- μm particle, 100- \AA pore; 75 μm \times 150 mm dimension; Thermo Scientific) held at 50 $^{\circ}\text{C}$. The solvent gradient was 0–110 min: 0–40% B; 110–117 min: 40–80% B; 117–120 min: 80% B; 300 $\text{nL}\cdot\text{min}^{-1}$; A: 0.1% formic acid, 2% acetonitrile; B: 0.1% formic acid, 80% acetonitrile. Ten μL of each high-pH fraction was injected by the autosampler on the Easy-nLC 1000 nano-UPLC system.

Protein identification from mass spectrometry data. Mass spectrometry was performed on an LTQ Orbitrap Elite mass spectrometer (Thermo Fisher Scientific) controlled by XCalibur (v.2.1.0) coupled to the Easy-nLC 1000 nano-UPLC system through a Thermo EasySpray interface. Each survey scan was analyzed inside the orbitrap at 60,000 resolving power in profile mode, followed by data-dependent collision-induced dissociation MS2 scans on the top 15 ions inside the ion trap. MS1 and MS2 target ion accumulations were 1×10^4 and 1×10^6 , respectively. Dynamic exclusion was set to 90 s. An MS1 lock mass of m/z 425.120025 was used. Protein identification was performed with ProLuCID (2) against a reverse-decoy database (human: Uniprot Reference Proteome Reviewed, Feb-09-2013, 20,241 entries; mouse: Uniprot Reference Proteome Reviewed, Feb-19-2013, 16,590 entries). Static cysteine carbamidomethylation (+57.02146 Da) modification and ≤ 3 variable methionine oxidation (+15.9949 Da), lysine acetylation (+42.0106 Da), serine/threonine/tyrosine phosphorylation (+79.9663 Da), or lysine ubiquitylation (+114.0403 Da) were allowed. Tryptic peptides within a 20-ppm mass window surrounding the candidate precursor mass were searched. Protein identifications were filtered by DTASelect (3), requiring $\leq 1\%$ global peptide false discovery rate and two unique peptides per protein. Modified and unmodified peptides are subjected to separate statistical filter in DTASelect v.2.0 with the `-modstat` parameter. Spectral counts were calculated in DTASelect. Additional protein identification was performed using MaxQuant (4) for comparison.

Computational workflow for $^2\text{H}_2\text{O}$ -labeling data analysis. The nonlinear fitting parameters utilized to deduce protein turnover rate were as follows. Orbitrap spectra were input to ProTurn after conversion

into [.mzML] format using MSConvert (5). ProTurn was instructed to select confidently identified peptides that were uniquely assigned to proteins, and to integrate the areas-under-curves within 60 ppm of the peptide mass at the retention time in the MS1 extracted ion chromatograph, as indicated by the scan number in the protein identification result. Savitzky-Golay filters were applied to the MS1 chromatographs prior to integration (6). Peptides shared by multiple proteins as indicated by the search engine (ProLuCID or MaxQuant) were discarded. In the mouse experiments, we accepted only peptides explicitly identified in at least 4 time points for kinetics calculation as a filter against false positive identifications and to minimize the effect of errors in isotope ratio measurements. Although more proteins may be quantified if the time-point requirement is relaxed, in our experience the statistics of low-abundance proteins does not contribute substantially to overall comparative analyses.

The integrated mass isotopomer fractional abundance information from every time point was fitted using the Nelder-Mead method (7) by ProTurn to optimize for k . The optimization results were independently verified by two data-fitting scripts, written in R and in MATLAB. Peptide isotopomer time-series were accepted if they fit to the model with $r \geq 0.9$, or alternatively with standard error of estimate $\leq 10\%$ in the mouse or a variable threshold $\leq 5-9\%$ in human, which permits a small proportion ($<10\%$) of well-fitted peptide isotopomers with low turnover rates. The error range of fitting for k at the isotopomer level is measured by $dk/dA_0 \times \sigma_A$, where σ_A is the residual sum of squares after optimization (vide infra). The turnover rate of a protein is reported as the median and the median absolute deviation of the turnover rates of all its constituent peptide isotopomers.

For the single-time-point analyses, the peptide isotopomer data were filtered without a priori knowledge of the true turnover rates from the full experimental dataset. For a fitting to be considered valid: (1) the coefficient of variance of the measured peptide isotopomer fractional abundance in the triplicate mass spectrometry experiments must be $\leq 10\%$; (2) the residual sum of squares of fitting must be $\leq 1.5\%$; and (3) the fitted turnover must lie within 0.5–3 half-lives at the sampling time.

For iBAQ label-free quantification in ProTurn, the integrated isotopomer peak areas were summed up as the peptide cluster area. Protein areas were defined as the sum of all peptide areas normalized to the total spectral intensity, then normalized to the potential number of tryptic peptides (six or more amino acids in length) that may be produced from the protein sequence (8).

Nonlinear model of ProTurn. The nonlinear model in ProTurn allows for large-scale proteome dynamics analysis in human as well as diverse animal models. Under gradual $^2\text{H}_2\text{O}$ enrichment, label

incorporation into proteins deviates from the first-order exponential decay function. We therefore derived a nonlinear function that resolves isotopomer shifts by accounting for both the rate constants of $^2\text{H}_2\text{O}$ enrichment and protein turnover. The gradual incorporation of isotope labels in a proteolytic peptide can be represented by the decrease in the fractional abundance of the 0th isotopomer, A_0 , i.e., the fraction of peptides devoid of any heavy isotopes. We followed the assumption that the decrease in fractional abundance of the unlabeled (0th) peptide isotopomer (dA_0/dt) upon ^2H incorporation follows the kinetics of protein pool replacement (9, 10). Thus the rate of decrease is strictly the result of protein turnover and follows first-order kinetics, where k is the protein turnover rate constant and $A_{0,max}$ is the fractional abundance of the 0th isotopomer in the newly-synthesized, labeled peptide, i.e., the amount of label that is entering the peptide pool. The component ($A_{0,max} - A_0$) therefore represents the difference between the steady-state label and the protein label at a particular time.

$$\frac{dA_0}{dt} = k(A_{0,max} - A_0) \quad (\text{S1})$$

The amount of label entering the protein is governed by the number of labeling sites on the peptide, N , the precursor enrichment level, p , and the natural fractional abundance of the 0th isotopomer prior to labeling, a :

$$A_{0,max} = a(1 - p)^N \quad (\text{S2})$$

In a simplified scenario where fast and constant precursor label enrichment can be achieved (e.g., in cell cultures following change of medium), $A_{0,max}$ is constant and represents the fractional abundance of the 0th isotopomer when the peptide is fully labeled as dictated by the precursor level, i.e., the fractional abundance when the peptide has reached the plateau and undergoes no additional changes. The resulting exponential decay equation reflects first-order kinetics:

$$A_0 = a + (A_{0,max} - a)(1 - e^{-kt}) \quad (\text{S3})$$

However, in most realistic labeling situations, p and therefore $A_{0,max}$ are time-dependent and a simple exponential decay equation no longer adequately describes the changes of A_0 . This is due to the fact that when an organism intakes $^2\text{H}_2\text{O}$, the pre-existing unlabeled H_2O predominates in molar ratio, and relative isotope abundance of ^2H rises slowly. We further reasoned that the time-dependent change of relative isotope abundance itself follows first-order kinetics with the steady-state level p_{ss} and the rate constant of k_p .

$$p = p_{ss}(1 - e^{-k_p t}) \quad (\text{S4})$$

Substituting **Equation S4** into **Equation S2**:

$$A_{0,max} = a \left(1 - p_{ss}(1 - e^{-k_p t})\right)^N \quad (\text{S5})$$

The differential equation for dA_0/dt could now be solved, after substituting **Equation S5** into **Equation S1** and performing binomial expansion on the resulting expression (11):

$$\frac{dA_0}{dt} = k \left(a \left(1 - p_{ss}(1 - e^{-k_p t})\right)^N - A_0 \right) \quad (\text{S6})$$

$$\frac{dA_0}{dt} = k \left(a \left((1 - p_{ss}) + p_{ss} e^{-k_p t} \right)^N - A_0 \right)$$

$$\frac{dA_0}{dt} = k \left(a \sum_{n=0}^N \binom{N}{n} (1 - p_{ss})^{N-n} (p_{ss} e^{-k_p t})^n - A_0 \right)$$

$$\frac{dA_0}{dt} = k a \left(\sum_{n=0}^N b_n e^{-n k_p t} \right) - A_0$$

$$b_n = \binom{N}{n} (1 - p_{ss})^{N-n} p_{ss}^n$$

Solving the differential equation:

$$A_0 = a \sum_{n=0}^N \left(\frac{k}{k - n k_p} b_n e^{-n k_p t} + \left(\frac{1}{N+1} - \frac{k}{k - n k_p} b_n \right) e^{-k t} \right) \quad (\text{S7})$$

Equation S7 fully describes the time-dependent change in A_0 as the result of labeling, and is a nonlinear function of five parameters:

- i. k , the turnover rate of the protein to which the peptide belongs. This is the parameter of interest.
- ii. p_{ss} , the plateau level of enrichment of $^2\text{H}_2\text{O}$ in the biological system. This parameter was readily measured from body fluid samples with gas chromatography-mass spectrometry.

- iii. k_p , the rate constant of the rise-to-plateau kinetics of body water $^2\text{H}_2\text{O}$ enrichment. This parameter could be acquired from fitting gas chromatography measurements of body fluid samples at regular time points following the initiation of labeling to **Equation S4**.
- iv. a , which represents the unlabeled fractional abundance of the 0th isotopomer of the particular peptide. The value of a could be readily calculated from the peptide sequence and the natural biological abundance of heavy isotopes of carbon, nitrogen, oxygen, and sulfur, using the formula:

$$a = (1 - 0.011)^{N_c}(1 - 0.00366)^{N_N}(1 - 0.00238)^{N_o}(1 - 0.0498)^{N_s}$$

N_C, N_N, N_O, N_S denote the number of carbon, nitrogen, oxygen, and sulfur atoms in the peptide, respectively.

- v. N , which represents the number of deuterium-accessible labeling sites on the peptide sequence. N could then be calculated as the sum of the known average accessible deuterium/tritium labeling sites on individual amino acids (N_{aa}) in mice, as has been reported in the literature (12). It may be seen from experimental data (**Supplemental Data 2**) that the values of a and N accurately predict the plateau values of A_o of identified peptides, which is given by $a \cdot (1 - p_{ss})^N$. The values of a and N may be further adjusted in cases of methionine oxidation, serine/threonine/tyrosine phosphorylation, lysine acetylation, and the lysine ubiquitination remnant diglycine, based on their respective atomic compositions.

The values for p_{ss} and k_p , for an experiment, together with the values of a and N for each individual peptide, were then substituted into **Equation S7**, which could now be fitted using the Nelder-Mead method (7) for the optimal value of k that minimizes the residual values between the model and the experimental data points. In systems where the target enrichment levels are quickly achieved ($k_p \gg k$) such as in mouse models, $A_{o,max}$ is effectively constant and the nonlinear model approaches a simple first-order exponential decay function. The nonlinear model is therefore applicable to both gradual and fast labeling experiments and can be used in both the mouse and human labeling studies.

In all cases of fitting, the standard error of fitting for each peptide time-series was estimated by:

$$\begin{aligned} \frac{dk}{dA_0} \sigma_A &= \sigma_k \\ \frac{dk}{dA_0} &= \frac{1}{a \sum_{n=0}^N \left(\frac{nk_p}{k(k-nk_p)} \frac{k}{k-nk_p} b_n (e^{-kt} - e^{-nk_p t}) - t \left(\frac{1}{N+1} - \frac{k}{k-nk_p} b_n \right) e^{-kt} \right)} \\ \sigma_k &= \frac{\sigma_A}{a \sum_{n=0}^N \left(\frac{nk_p}{k(k-nk_p)} \frac{k}{k-nk_p} b_n (e^{-kt} - e^{-nk_p t}) - t \left(\frac{1}{N+1} - \frac{k}{k-nk_p} b_n \right) e^{-kt} \right)} \end{aligned} \quad (\text{S8})$$

Since **Equation S8** is a function of time, we estimated error for each fitting where A_0 was most sensitive to the change of k among the time points where experimental data exist. The upper limit and the lower limit of k were defined as $k + \sigma_k$ and $k^2/(k + \sigma_k)$, respectively. The minimized sum of residual squares (σ_A) also allowed for an evaluation of the goodness-of-fit of the function. Fitting accuracy in the nonlinear regression used was not in some cases reflected by the coefficient of determination alone. Slow turnover peptides with relatively gentle curves had low coefficients of determination even when residuals from the curve were minimal and the kinetics curve trajectory was apparent. This is because the residual variance approached the data point variance. To ensure reliable data points are retained and at the same time filter out unreliable data, we additionally calculated the standard error of estimate (SE) of the fitted data:

$$r = \sqrt{1 - \frac{\sigma_A}{(\sum_i (A_{0,t=i} - \bar{A}))^2}}$$

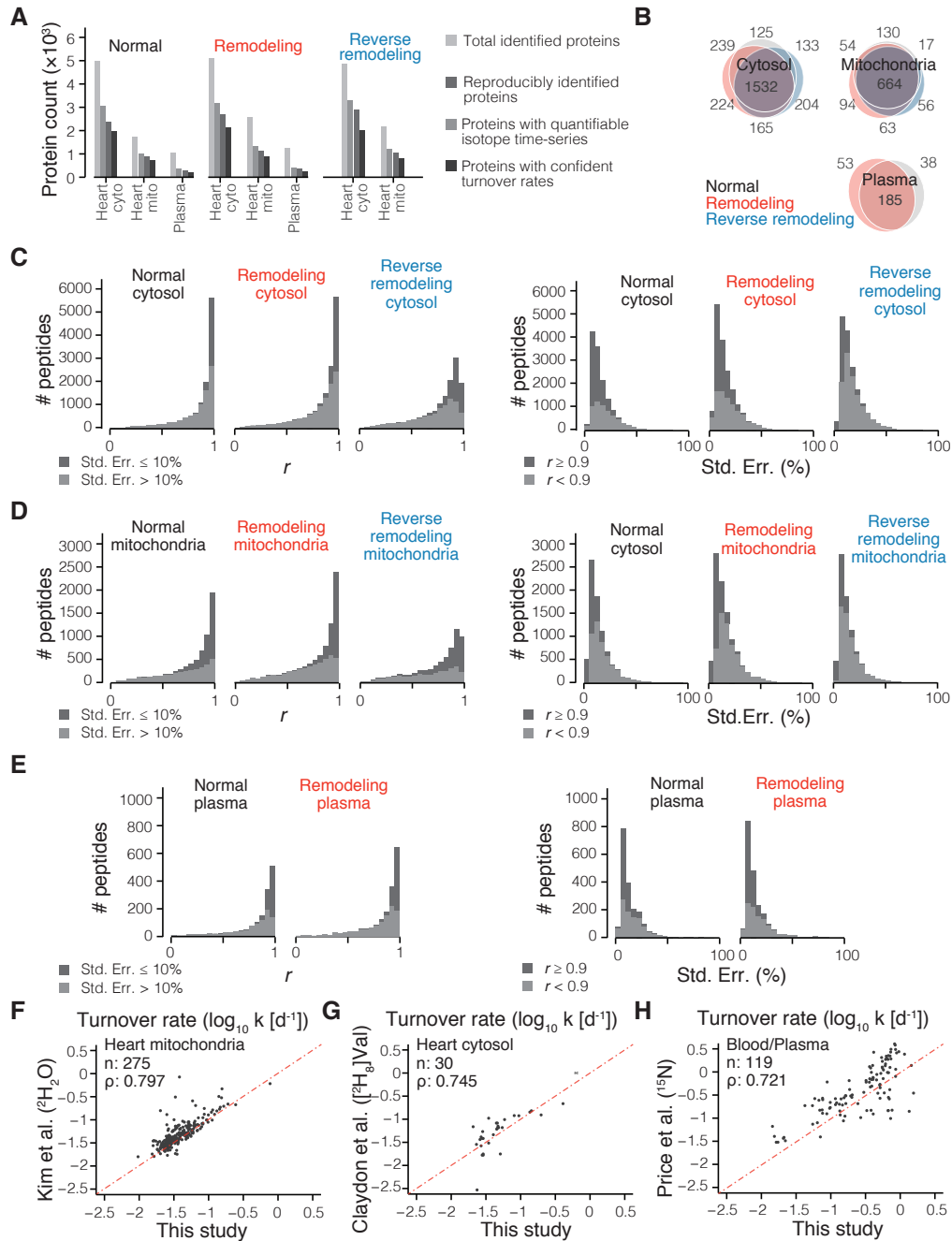
$$SE = \sqrt{\frac{\sigma_A}{v}}$$

For fitted curves with the quasi-constant enrichment scheme in the mouse experiments, peptides that showed $r \geq 0.9$ or $SE \leq 10\%$ were accepted. In human labeling, enrichment levels reached different plateaux in each subject, causing intrinsic spectral abundance variability to affect fitting to various degrees especially for the low-turnover curves that were permitted by standard errors, i.e., data from individuals with lower p_{ss} values were more variable because on average less ^2H atoms were incorporated into proteins. We therefore used a variable standard error filter that varied between 4 to 9% for each subject. These values were empirically determined to maximize the number of retained well-fitted peptides while minimizing peptide-to-peptide variability within a given protein.

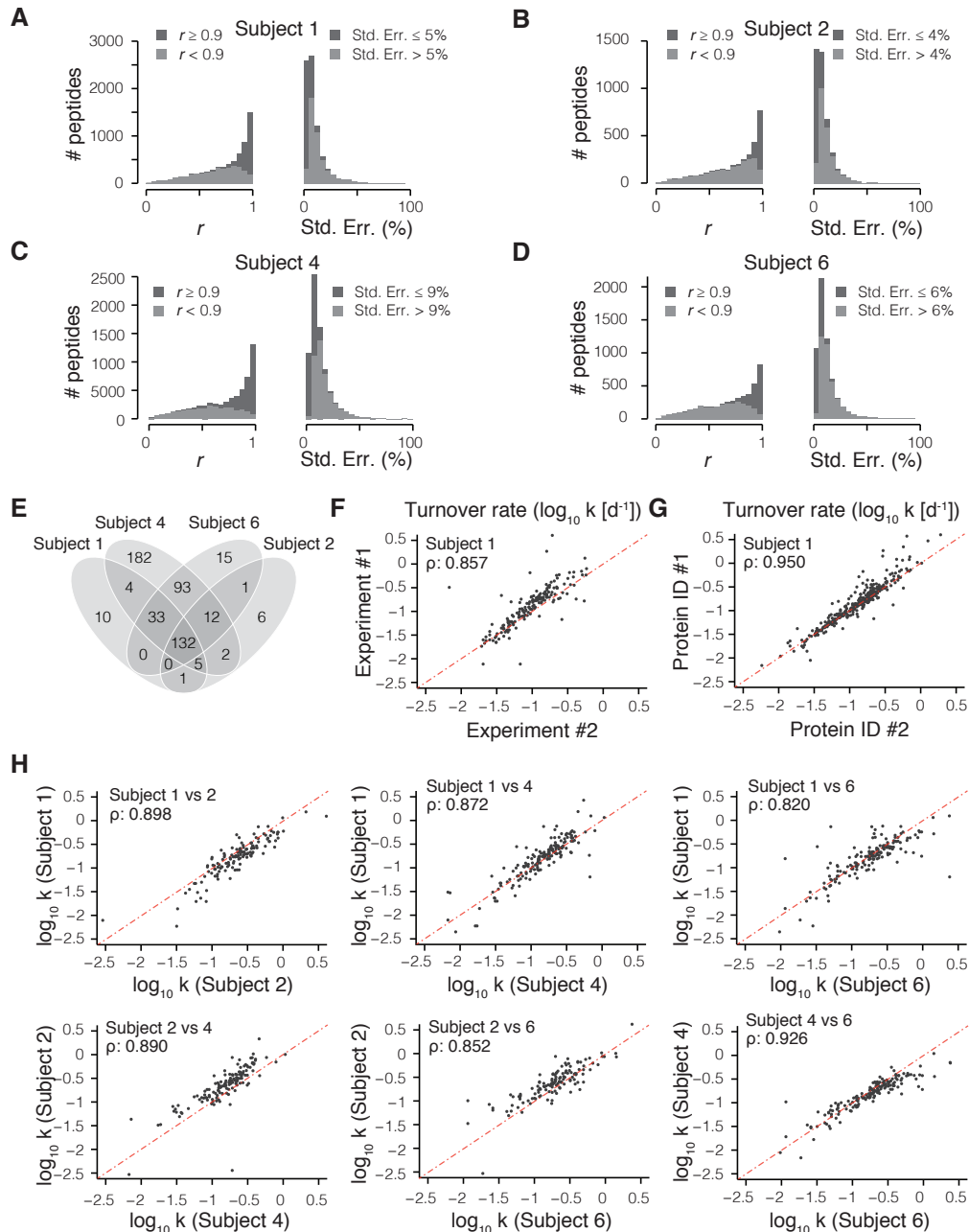
The significance of protein kinetics comparison between two samples was evaluated on multiple levels. On the peptide isotopomer abundance level, every non-zero time point-fractional label coordinate between proteins from two samples was compared using Kolmogorov-Smirnov and Mann-Whitney-

Wilcoxon statistics. On the isotopomer time-series level, we compared the value (optimized k) and deviation (optimized σ_k) of each peptide-sequence pair between proteins of two samples using the Welch's t test. The minimal pairwise fitting error significance (maximal P) among all peptide-sequence pairs were reported as its P value (P_{MPFE}). Lastly on the peptide distribution level, the Mann-Whitney-Wilcoxon test was performed on every protein pair in any two samples each with three or more confidently fitted peptides and reported as its P value (P_{PD}).

Supplemental Figures:



Supplemental Figure S1. Nonlinear fitting of 2H_2O labeling data in mouse. (A) The number of proteins that were identified and quantified in each sample. (B) The overlap of proteins with confident turnover in normal and disease mice. (C–E) The goodness-of-fit (r) and standard error of estimate (Std. Err.) of the turnover rate fitting by the nonlinear model implemented in ProTurn, for each quantified peptide isotopomer in (C) mouse heart cytosol, (D) mouse heart mitochondria, and (E) mouse plasma. The method modeled the time-evolution of 35–50% of all peptide isotopomer series precisely. (F–H) The correlation between the turnover rates of common proteins analyzed in this study and three previous studies using 2H_2O , $[^2H_8]$ -valine and ^{15}N tracers (9, 13, 14).



Supplemental Figure S2. $^2\text{H}_2\text{O}$ -labeling and data fitting in four healthy human subjects. (A-D) Histograms of goodness-of-fit of the nonlinear fitting model in healthy human subject 1, 2, 4, and 6. Only peptides explicitly identified in ≥ 4 time points and containing quantifiable mass isotopomer information are included. In these subjects, the nonlinear fitting method implemented in ProTurn modeled at least 35% of peptides closely ($r \geq 0.9$ or standard error of estimate of 4 to 9%). **(E)** Venn diagram of the overlap of protein species with confident turnover rates. **(F)** Scatter plot and Spearman's correlation coefficient of turnover rates, showing the reproducibility of protein turnover rates in two labeling procedures and MS experiments conducted on the same subject (Subject 1) six months apart. Each data point represents a commonly quantified individual protein. **(G)** Scatter plot and Spearman's correlation coefficient of turnover rates from the same sample (Subject 1) when processed using two different protein identification workflows (ProLuCID and MaxQuant). **(H)** Scatter plots and Spearman's correlation coefficient of turnover rates of proteins commonly identified in any pairwise combination of the four subjects.

Supplemental Data

Supplemental Data 1 [.xlsx] | Protein turnover rates in each sample.

Supplemental Data 2 [.pdf] | Example fitting evidence for peptide isotopomers in human. All fitting data can be found at [<http://www.heartproteome.org/proturn/supplemental>].

References:

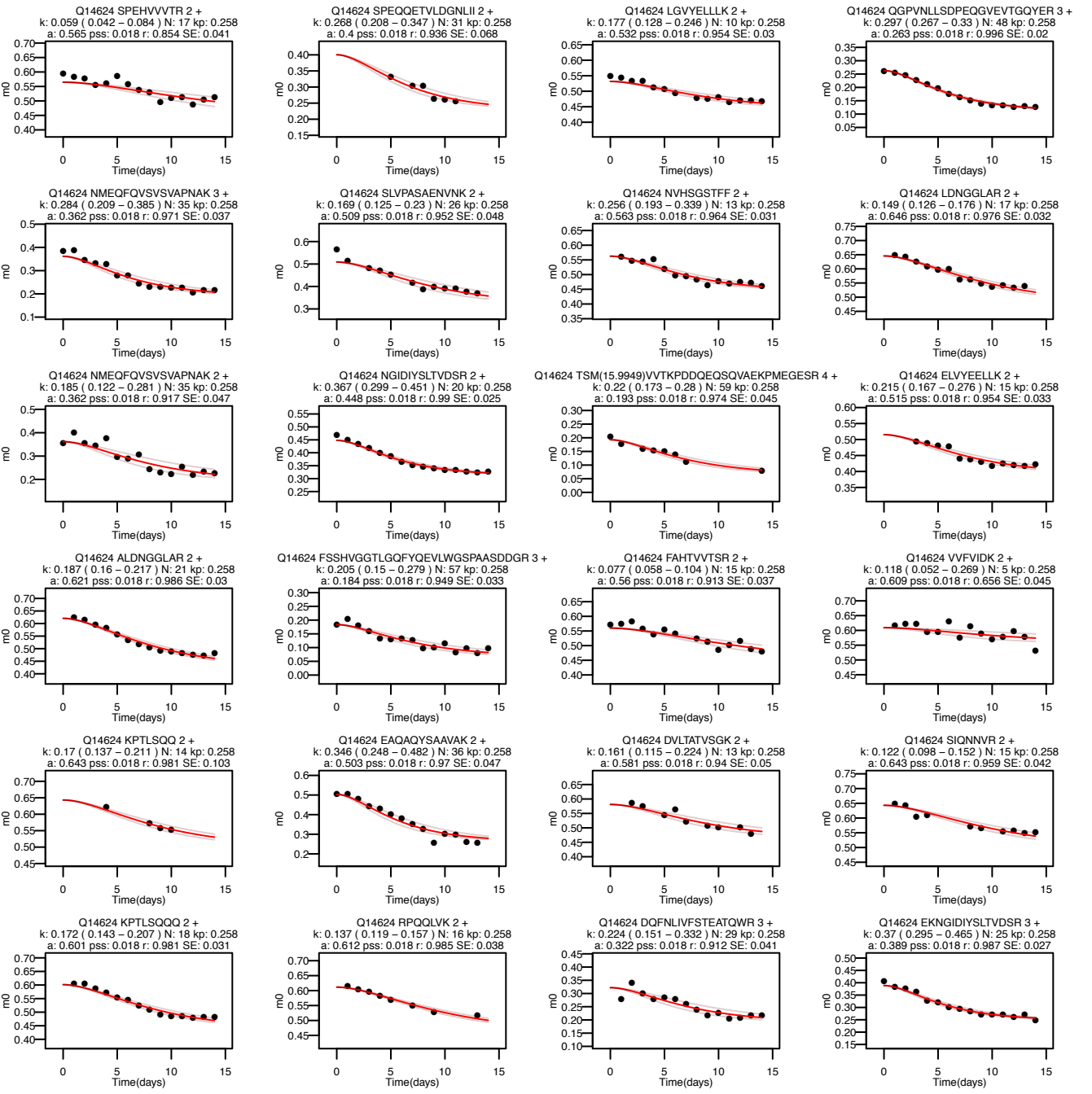
1. Wisniewski, J.R., Zougman, A., Nagaraj, N., and Mann, M. 2009. Universal sample preparation method for proteome analysis. *Nat Methods* 6:359-362.
2. Xu, T., Venable, J.D., Park, S.K., Cociorva, D., Lu, B., Liao, L., Wohlschlegel, J., Hewel, J., and Yates, J.R., 3rd. 2006. ProLuCID, a fast and sensitive tandem mass spectra-based protein identification program. *Mol Cell Proteomics* 5:S174.
3. Tabb, D.L., McDonald, W.H., and Yates, J.R., 3rd. 2002. DTASelect and Contrast: tools for assembling and comparing protein identifications from shotgun proteomics. *J Proteome Res* 1:21-26.
4. Cox, J., and Mann, M. 2008. MaxQuant enables high peptide identification rates, individualized p.p.b.-range mass accuracies and proteome-wide protein quantification. *Nat Biotechnol* 26:1367-1372.
5. Chambers, M.C., Maclean, B., Burke, R., Amodei, D., Ruderman, D.L., Neumann, S., Gatto, L., Fischer, B., Pratt, B., Egertson, J., et al. 2012. A cross-platform toolkit for mass spectrometry and proteomics. *Nat Biotechnol* 30:918-920.
6. Savitzky, A., and Golay, M.J.E. 1964. Smoothing and differentiation of data by simplified least squares procedures. *Analytical Chemistry* 36:1627-1639.
7. Nelder, J.A., and Mead, R. 1965. A simplex-method for function minimization. *Computer Journal* 7:308-313.
8. Schwanhauser, B., Busse, D., Li, N., Dittmar, G., Schuchhardt, J., Wolf, J., Chen, W., and Selbach, M. 2011. Global quantification of mammalian gene expression control. *Nature* 473:337-342.
9. Kim, T.Y., Wang, D., Kim, A.K., Lau, E., Lin, A.J., Liem, D.A., Zhang, J., Zong, N.C., Lam, M.P., and Ping, P. 2012. Metabolic labeling reveals proteome dynamics of mouse mitochondria. *Mol Cell Proteomics* 11:1586-1594.
10. Price, J.C., Holmes, W.E., Li, K.W., Floreani, N.A., Neese, R.A., Turner, S.M., and Hellerstein, M.K. 2012. Measurement of human plasma proteome dynamics with (2)H(2)O and liquid chromatography tandem mass spectrometry. *Anal Biochem* 420:73-83.
11. Stewart, J. 1999. *Calculus - Early Transcendentals*. Pacific Grove, CA: Brooks/Cole Pub Co.
12. Commerford, S.L., Carsten, A.L., and Cronkite, E.P. 1983. The distribution of tritium among the amino acids of proteins obtained from mice exposed to tritiated water. *Radiat Res* 94:151-155.
13. Claydon, A.J., Ramm, S.A., Pennington, A., Hurst, J.L., Stockley, P., and Beynon, R. 2012. Heterogenous turnover of sperm and seminal vesicle proteins in the mouse revealed by dynamic metabolic labeling. *Mol Cell Proteomics* 11:M111 014993.
14. Price, J.C., Guan, S., Burlingame, A., Prusiner, S.B., and Ghaemmaghami, S. 2010. Analysis of proteome dynamics in the mouse brain. *Proc Natl Acad Sci U S A* 107:14508-14513.

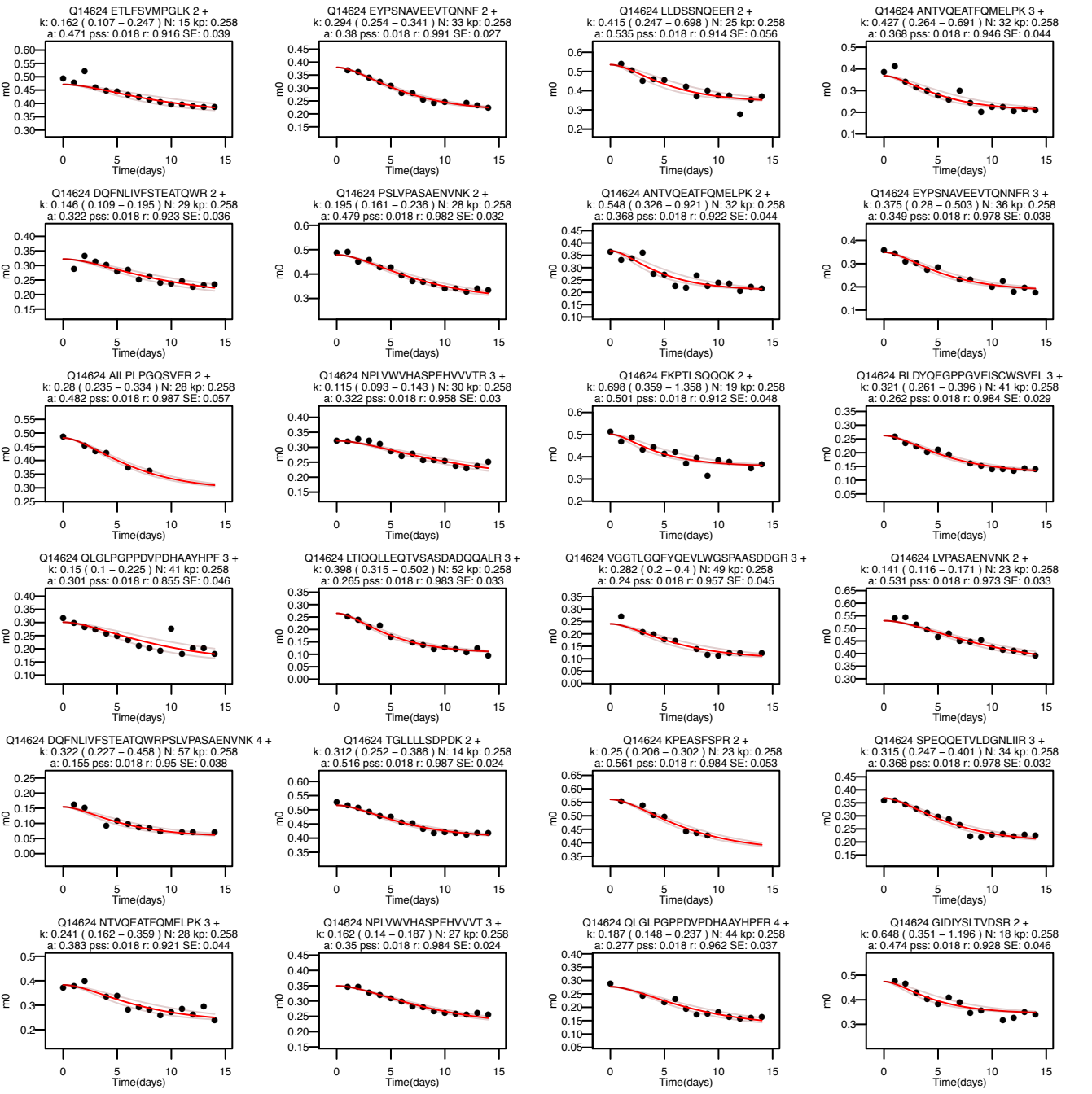
Supplemental Data 2:

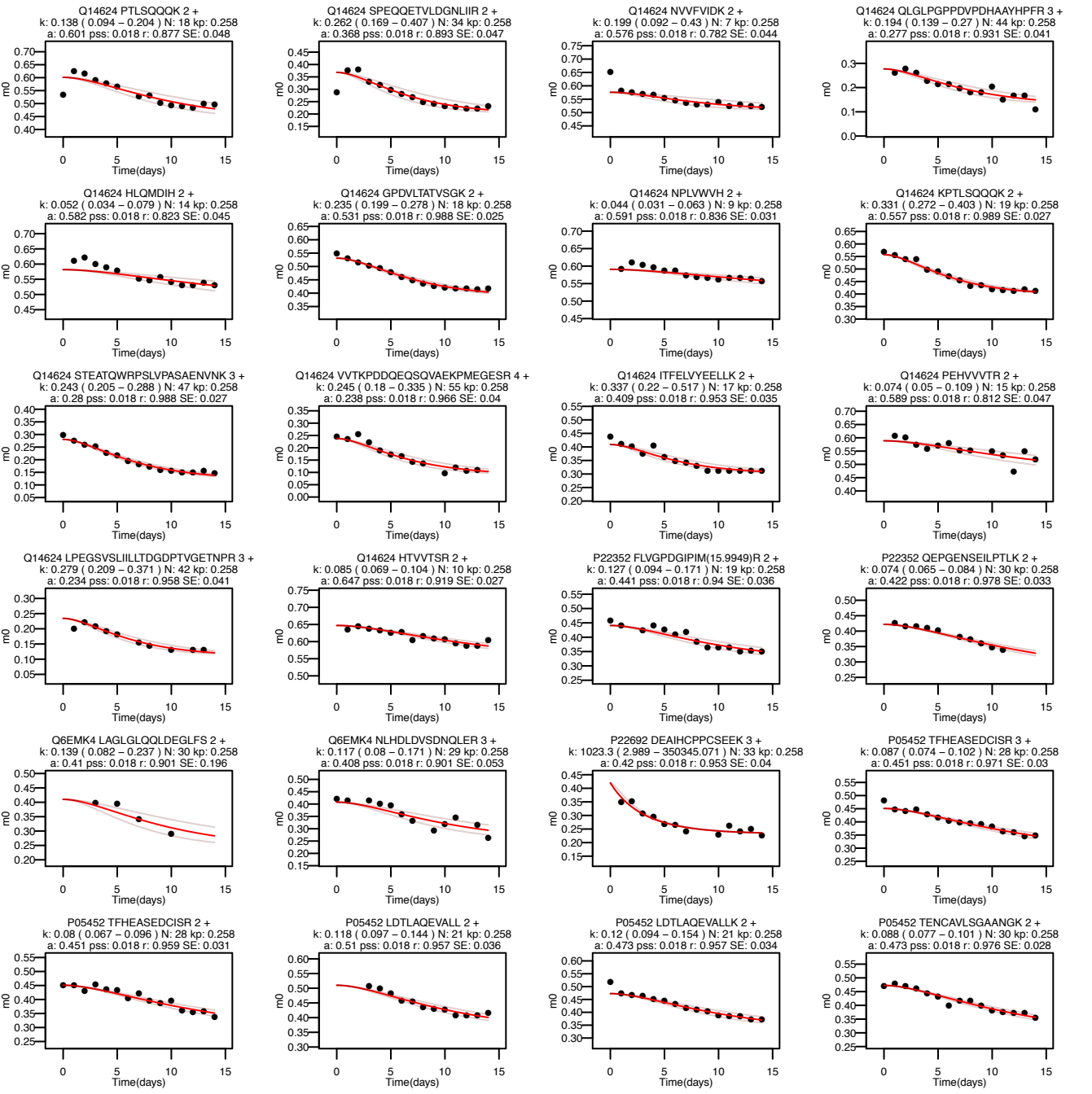
This file contains the data fitting evidence of 120 peptides from each of Human Subject 1, 2, 4, and 6.

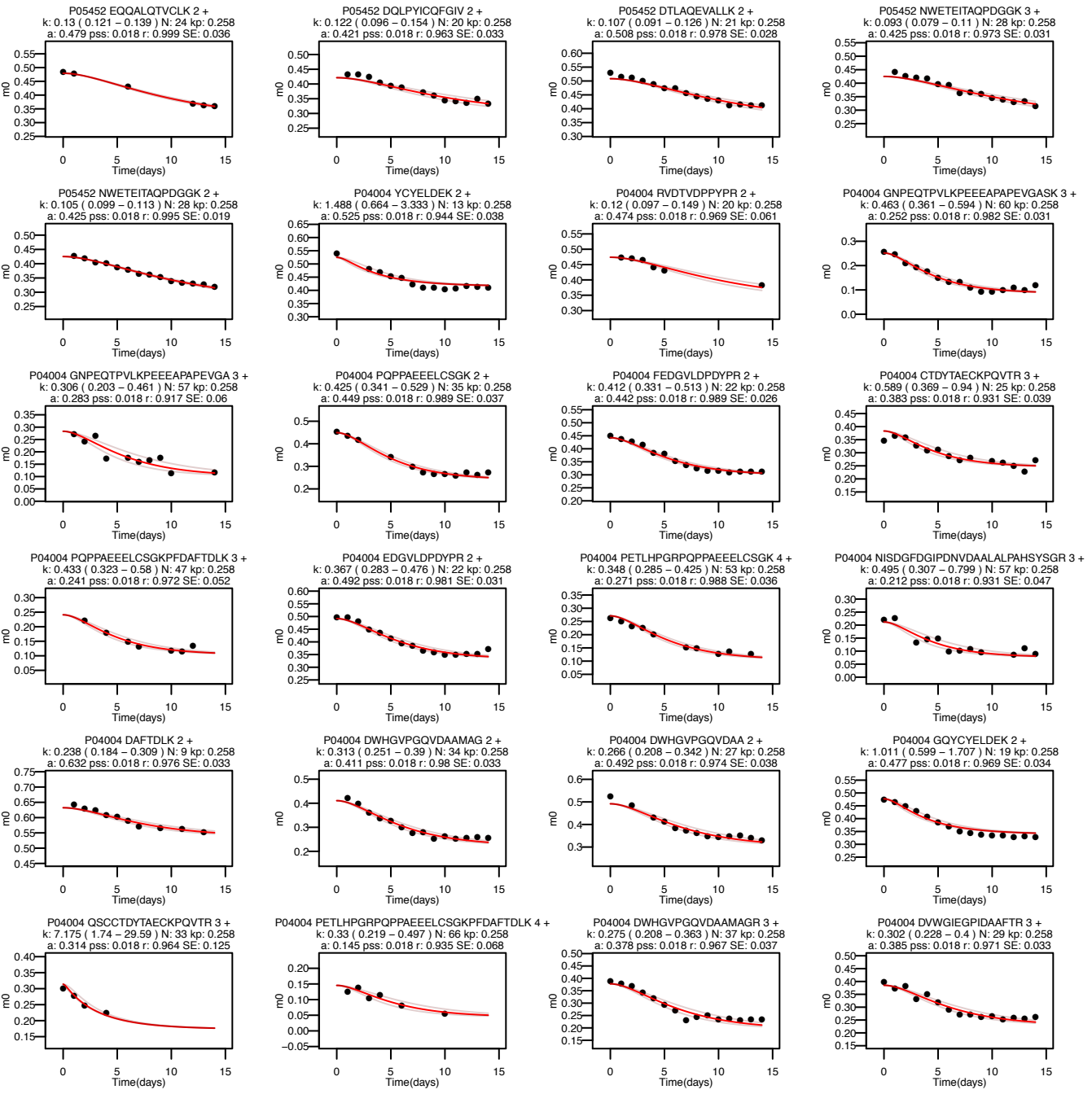
All fitting evidences can be downloaded at:

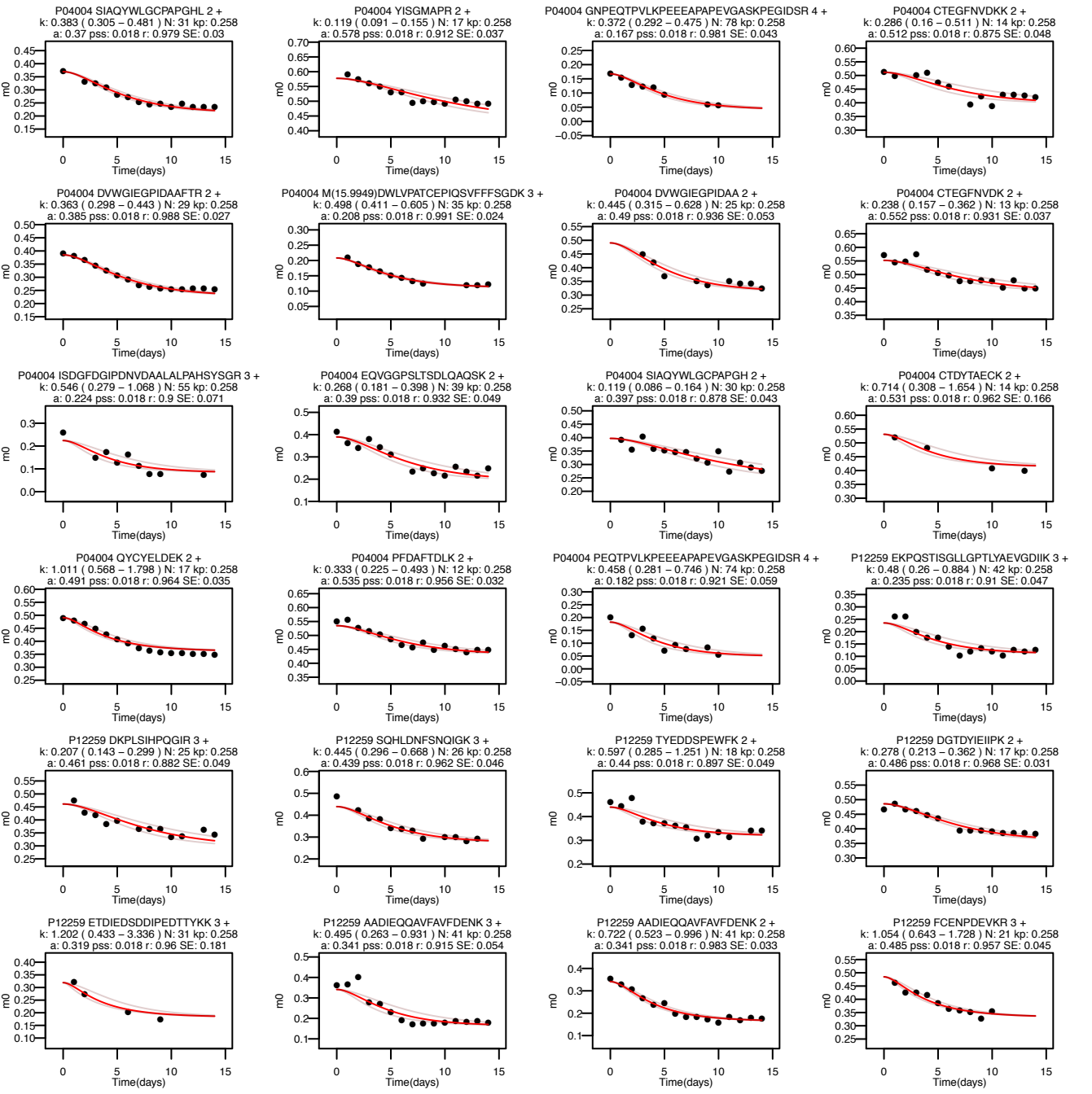
[<http://www.heartproteome.org/proturn/supplemental>]

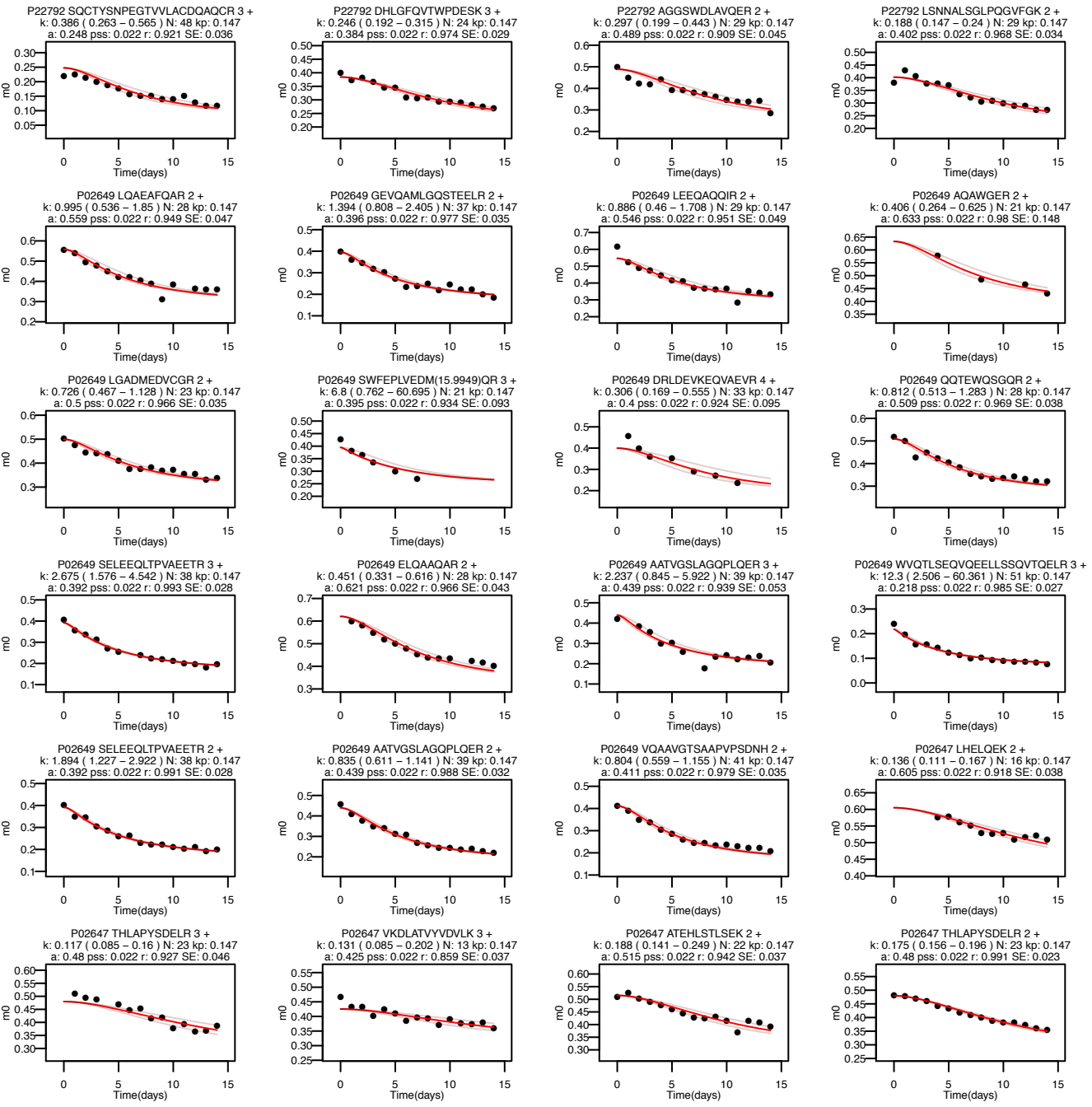


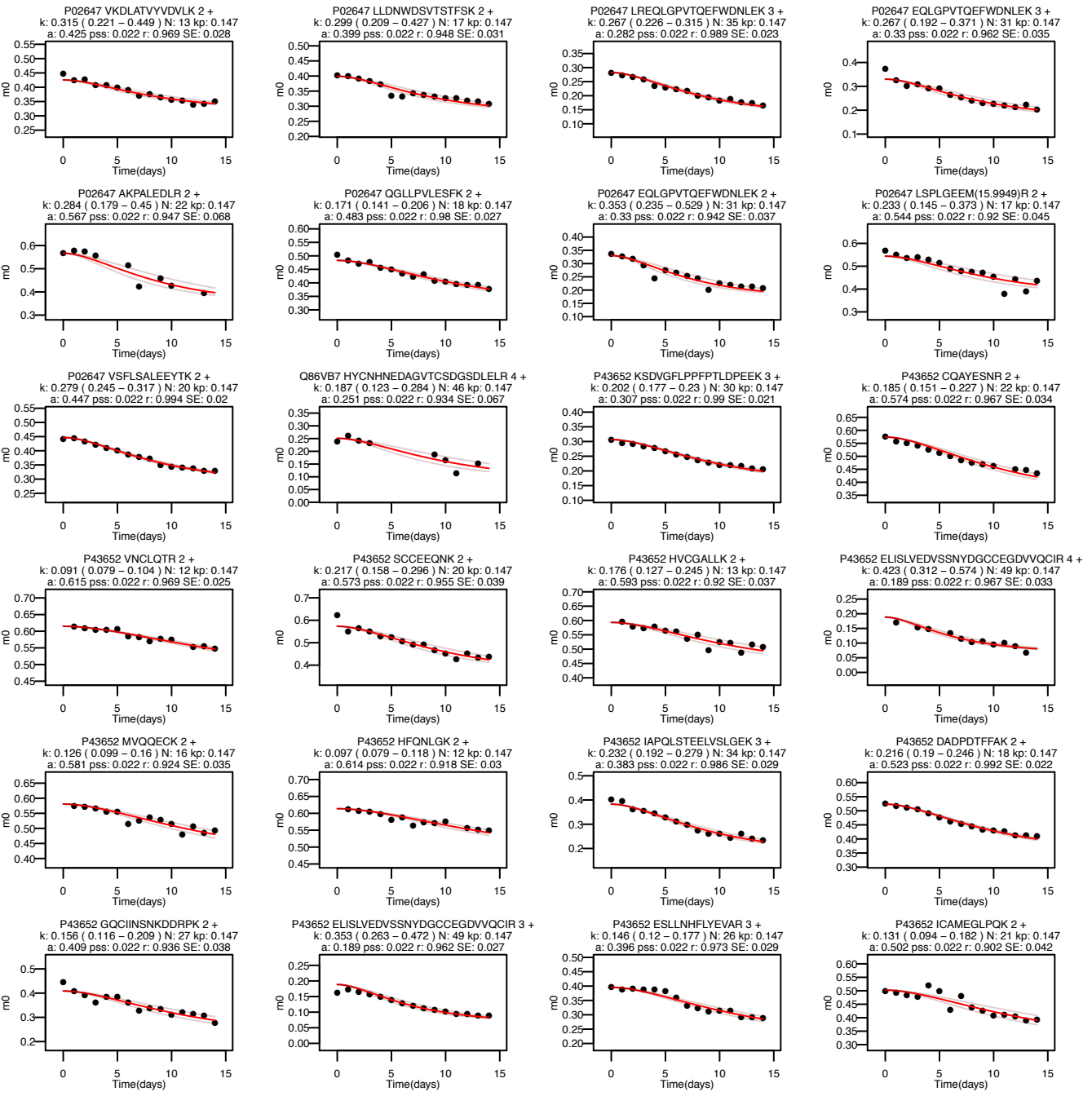


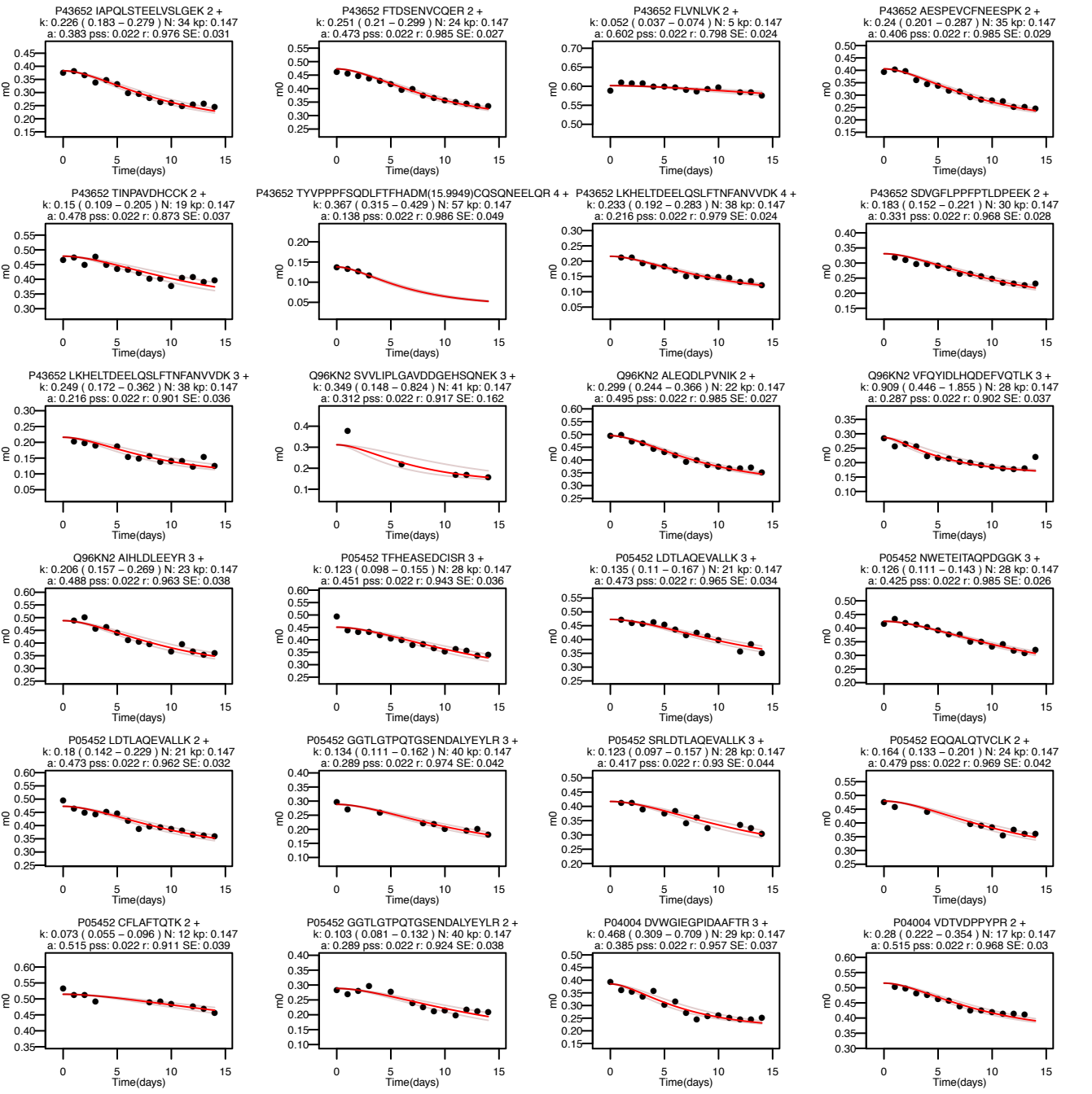


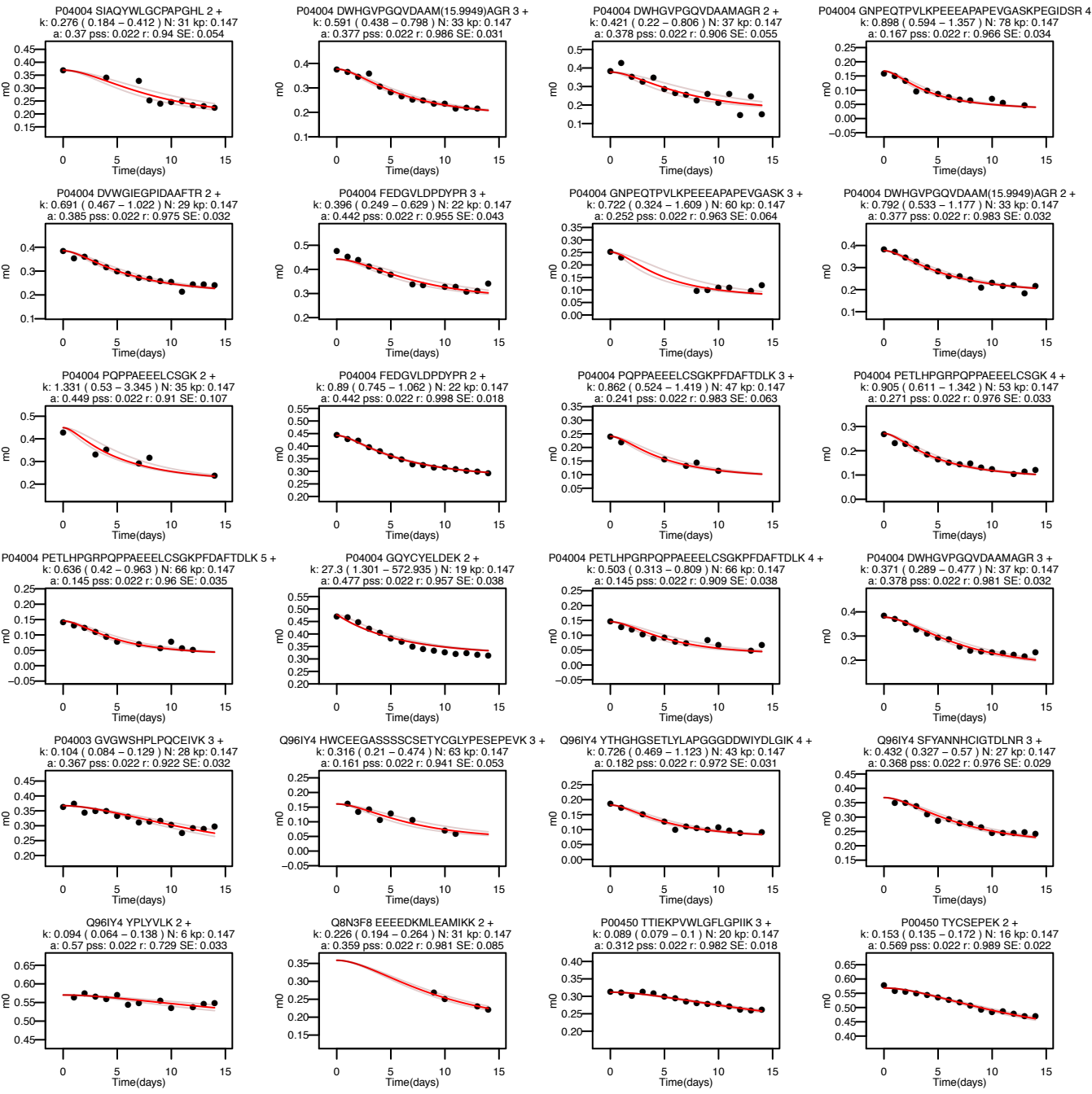


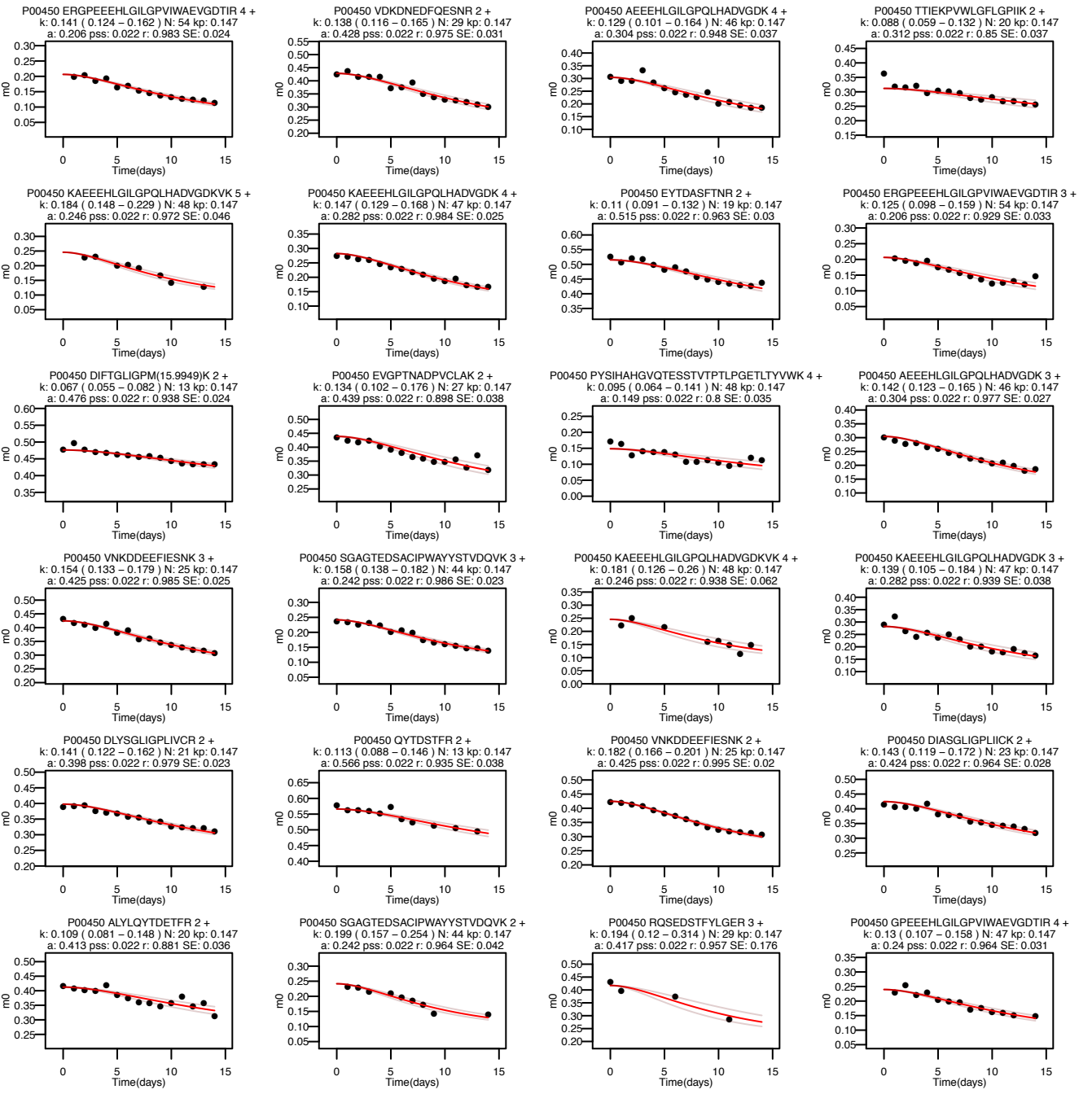


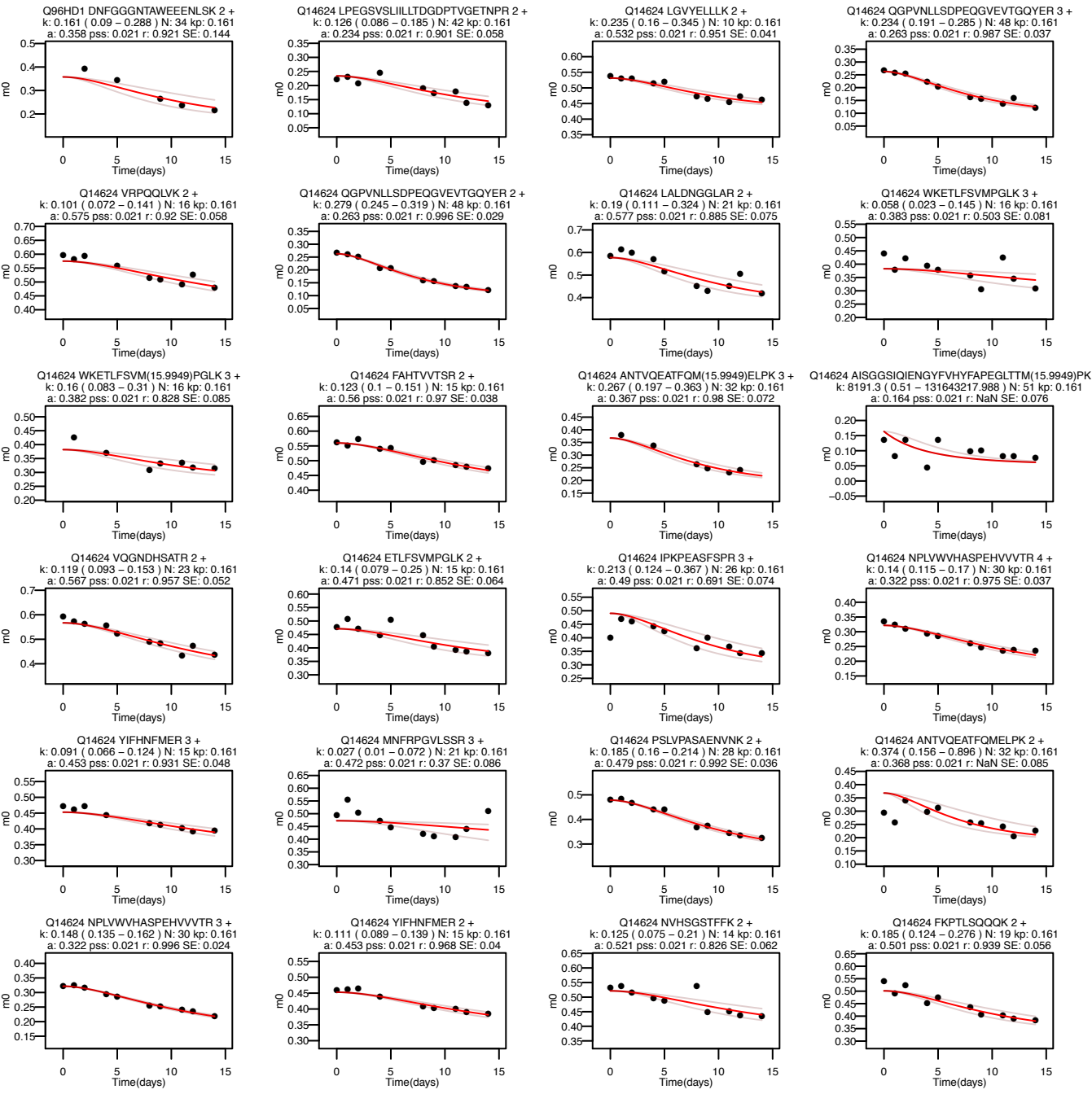


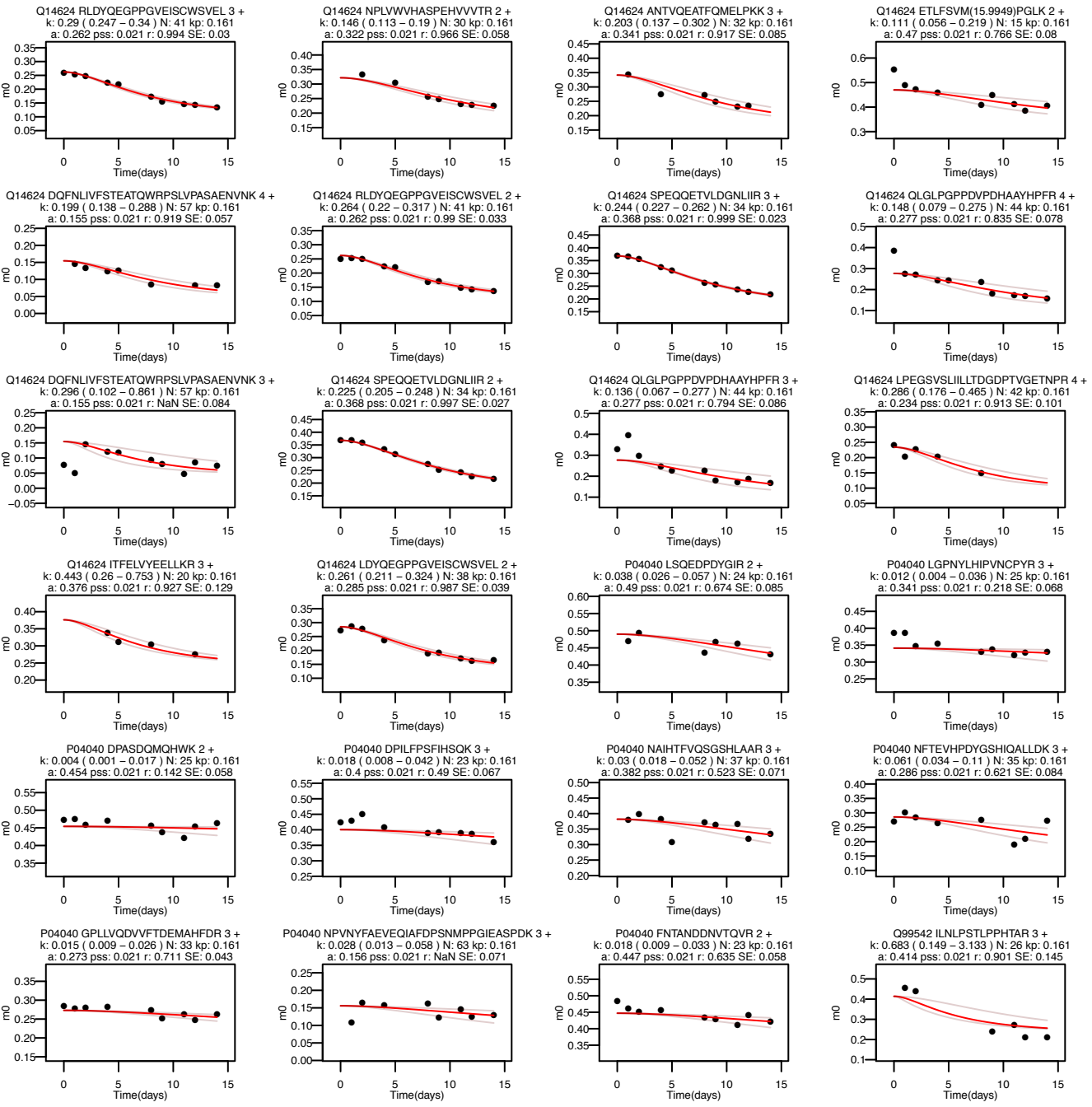


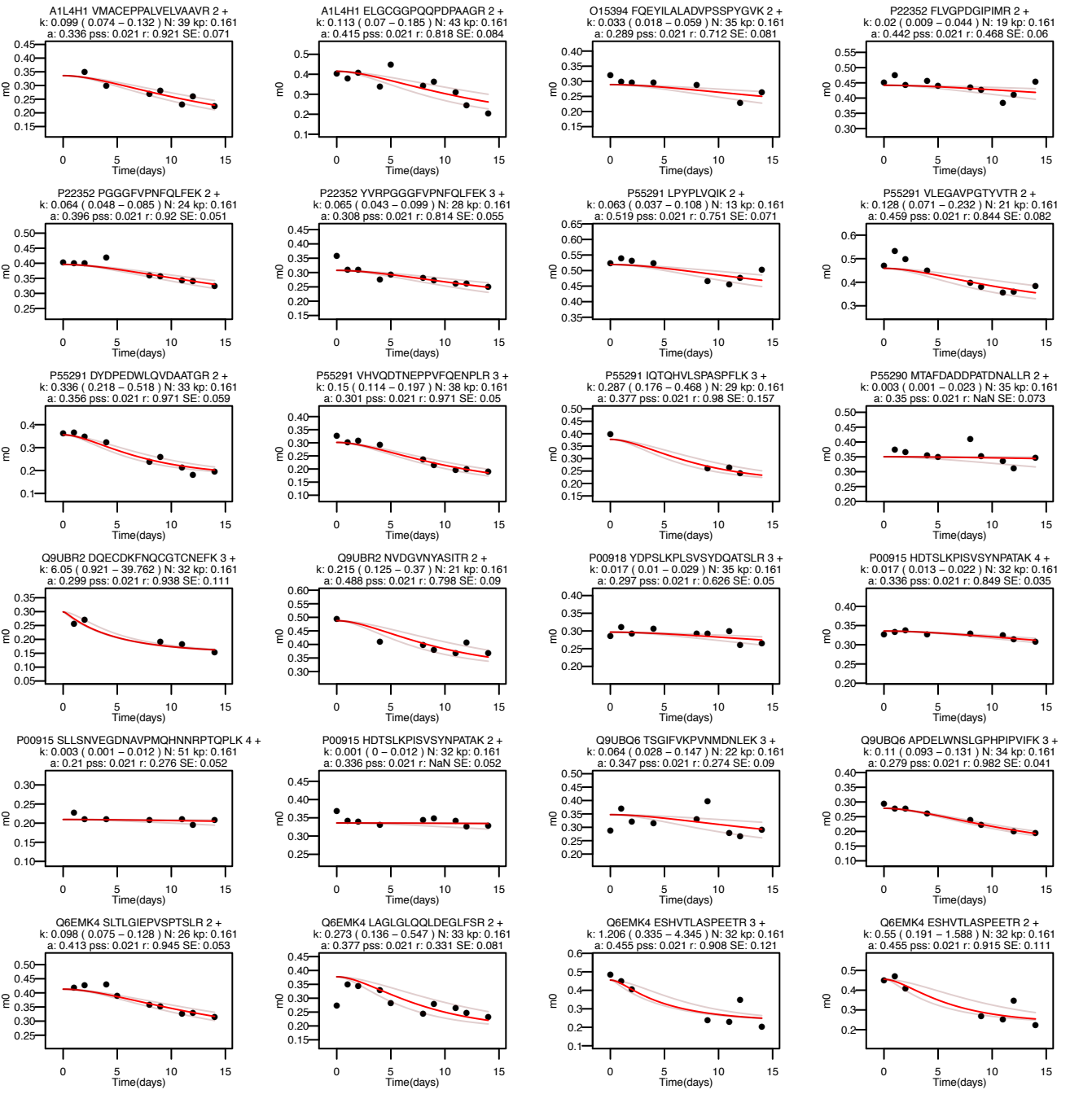


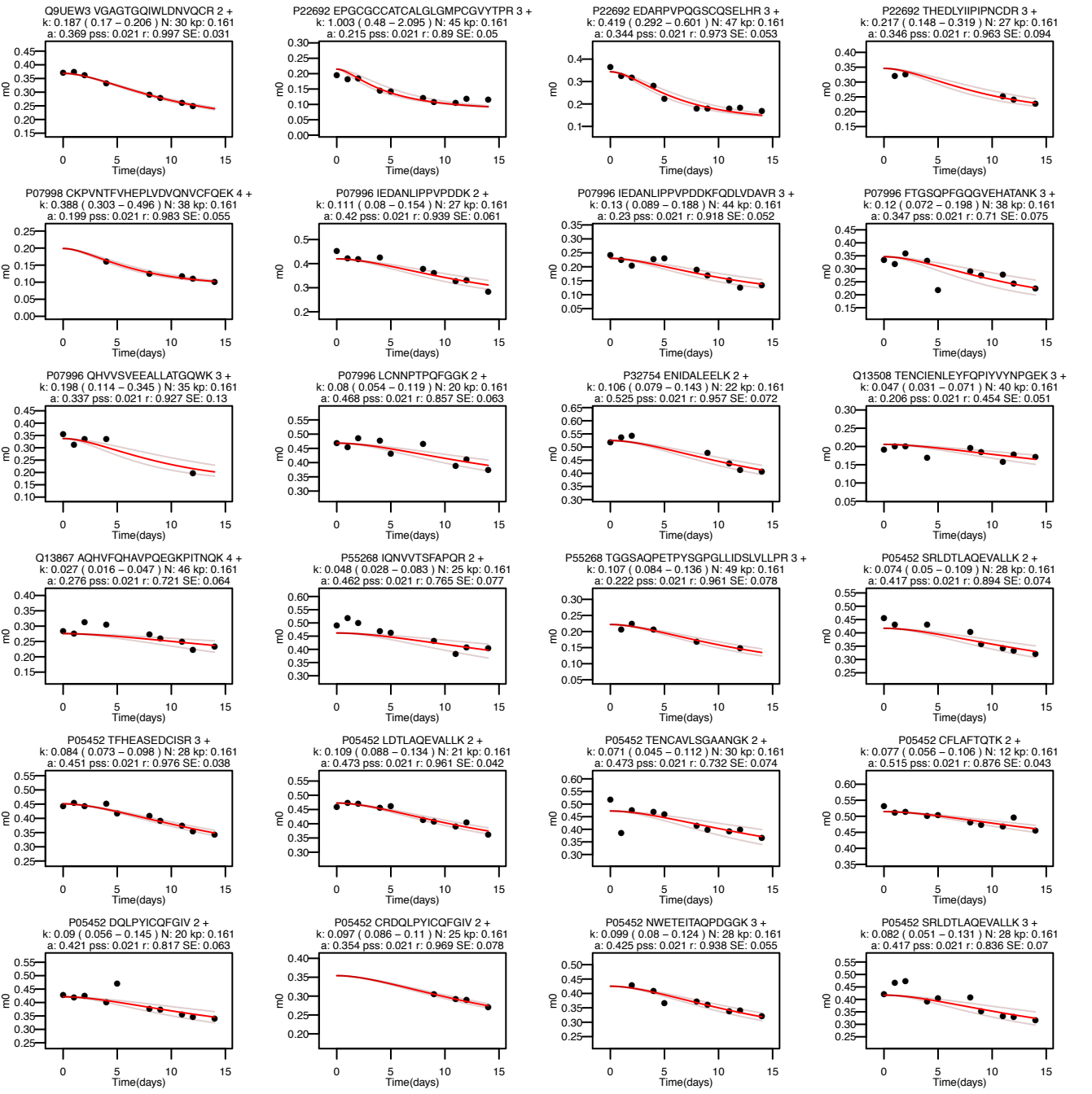


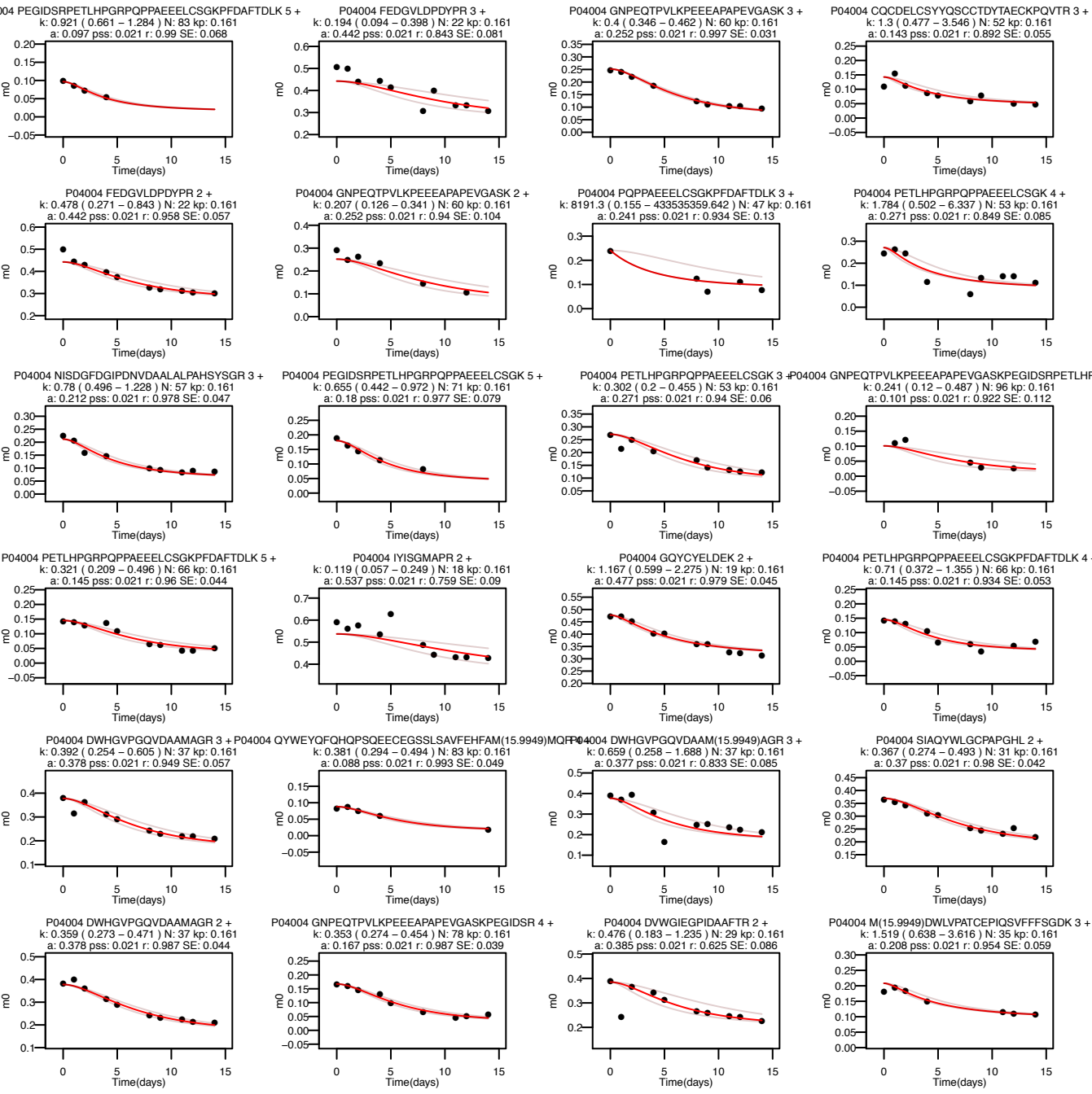




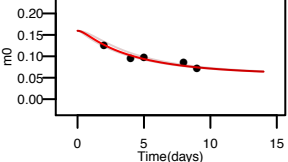




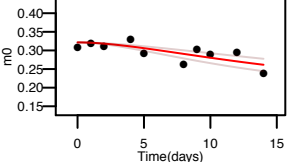




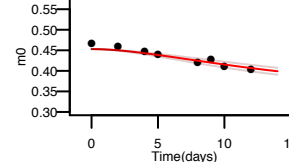
07037 NWAVTQPDNWHHELGGSEDCVEVQPDGR 4 +
k: 2.706 (1.172 - 6.247) N: 63 kp: 0.159
a: 0.16 pss: 0.016 r: 0.956 SE: 0.064



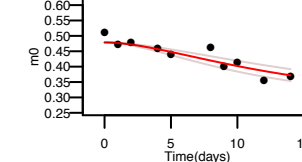
Q14624 NPLVWVHASPEHVVVTR 4 +
k: 0.081 (0.051 - 0.127) N: 30 kp: 0.159
a: 0.322 pss: 0.016 r: 0.717 SE: 0.056



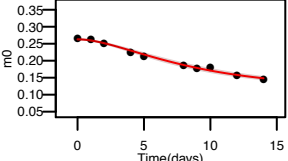
Q14624 YIFHNFEMER 3 +
k: 0.105 (0.079 - 0.14) N: 15 kp: 0.159
a: 0.453 pss: 0.016 r: 0.939 SE: 0.043



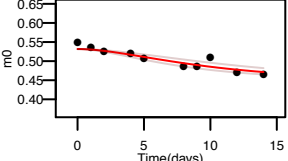
Q14624 PSLVPAASAENVK 2 +
k: 0.123 (0.084 - 0.179) N: 28 kp: 0.159
a: 0.479 pss: 0.016 r: 0.908 SE: 0.058



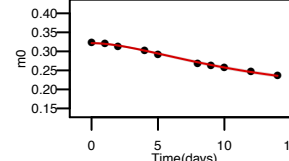
Q14624 QGPVNLSDPEQGVVETGQYER 3 +
k: 0.242 (0.213 - 0.275) N: 48 kp: 0.159
a: 0.263 pss: 0.016 r: 0.995 SE: 0.026



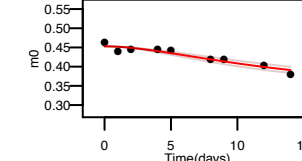
Q14624 LGVYELLK 2 +
k: 0.232 (0.138 - 0.388) N: 10 kp: 0.159
a: 0.532 pss: 0.016 r: 0.915 SE: 0.043



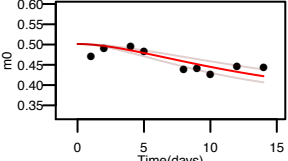
Q14624 NPLVWVHASPEHVVVTR 3 +
k: 0.162 (0.152 - 0.172) N: 30 kp: 0.159
a: 0.322 pss: 0.016 r: 0.998 SE: 0.018



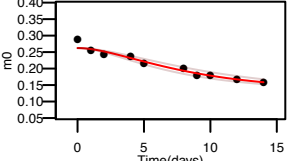
Q14624 YIFHNFEMER 2 +
k: 0.137 (0.103 - 0.183) N: 15 kp: 0.159
a: 0.453 pss: 0.016 r: 0.95 SE: 0.039



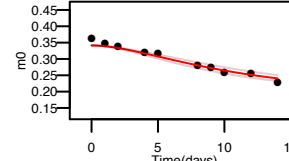
Q14624 FKPTLSQQQK 2 +
k: 0.121 (0.08 - 0.182) N: 19 kp: 0.159
a: 0.501 pss: 0.016 r: 0.731 SE: 0.058



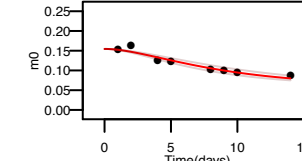
Q14624 RLDYQEGPPGVEISCWSVEL 3 +
k: 0.263 (0.188 - 0.367) N: 41 kp: 0.159
a: 0.262 pss: 0.016 r: 0.968 SE: 0.042



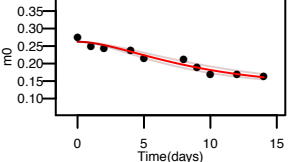
Q14624 ANTVEATFQMELPKK 3 +
k: 0.184 (0.142 - 0.24) N: 32 kp: 0.159
a: 0.341 pss: 0.016 r: 0.976 SE: 0.04



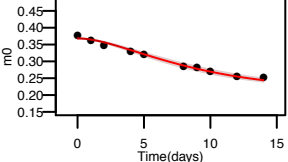
Q14624 DQFNLVFSTEATQWRPSLVPAASAENVK 4 +
k: 0.226 (0.165 - 0.309) N: 57 kp: 0.159
a: 0.155 pss: 0.016 r: 0.963 SE: 0.042



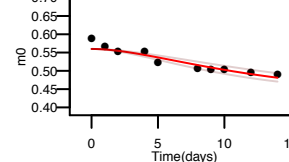
Q14624 RLDYQEGPPGVEISCWSVEL 2 +
k: 0.238 (0.175 - 0.323) N: 41 kp: 0.159
a: 0.262 pss: 0.016 r: 0.966 SE: 0.04



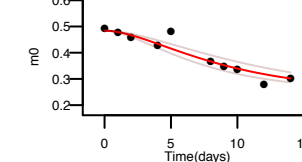
Q14624 SPEQQTVDLGNLIIR 3 +
k: 0.247 (0.212 - 0.289) N: 34 kp: 0.159
a: 0.368 pss: 0.016 r: 0.992 SE: 0.03



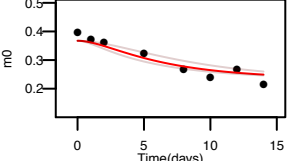
Q14624 FAHTVVTSR 2 +
k: 0.147 (0.104 - 0.207) N: 15 kp: 0.159
a: 0.56 pss: 0.016 r: 0.933 SE: 0.045



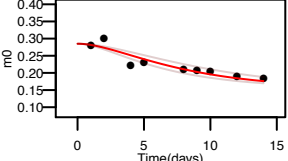
Q14624 AEAQAQYSAAVAK 2 +
k: 0.231 (0.153 - 0.349) N: 57 kp: 0.159
a: 0.484 pss: 0.016 r: 0.945 SE: 0.065



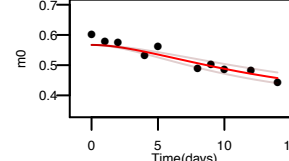
Q14624 ANTVEATFQM(15.9949)ELPK 3 +
k: 0.581 (0.265 - 1.277) N: 28 kp: 0.159
a: 0.367 pss: 0.016 r: 0.946 SE: 0.072



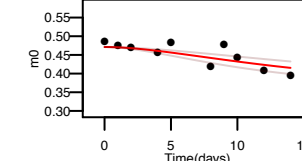
Q14624 LDYQEGPPGVEISCWSVEL 2 +
k: 0.299 (0.188 - 0.475) N: 38 kp: 0.159
a: 0.285 pss: 0.016 r: 0.926 SE: 0.054



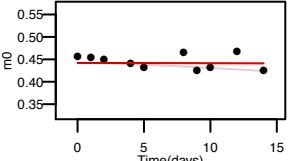
Q14624 VQGNDSATR 2 +
k: 0.129 (0.092 - 0.183) N: 23 kp: 0.159
a: 0.567 pss: 0.016 r: 0.932 SE: 0.055



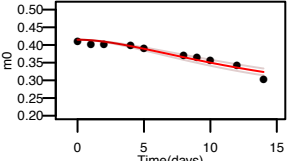
Q14624 ETLFVMPGLK 2 +
k: 0.104 (0.059 - 0.184) N: 15 kp: 0.159
a: 0.471 pss: 0.016 r: 0.779 SE: 0.058



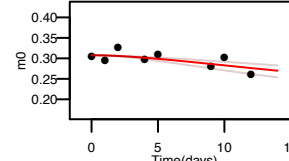
P22352 FLVPGDGIPIMR 2 +
k: 0.001 (0 - 0.019) N: 19 kp: 0.159
a: 0.442 pss: 0.016 r: NaN SE: 0.052



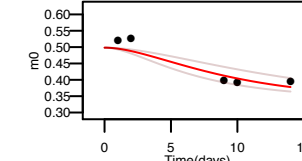
P22352 NSCPPTSSELLGTDSTR 2 +
k: 0.113 (0.092 - 0.138) N: 29 kp: 0.159
a: 0.415 pss: 0.016 r: 0.959 SE: 0.039

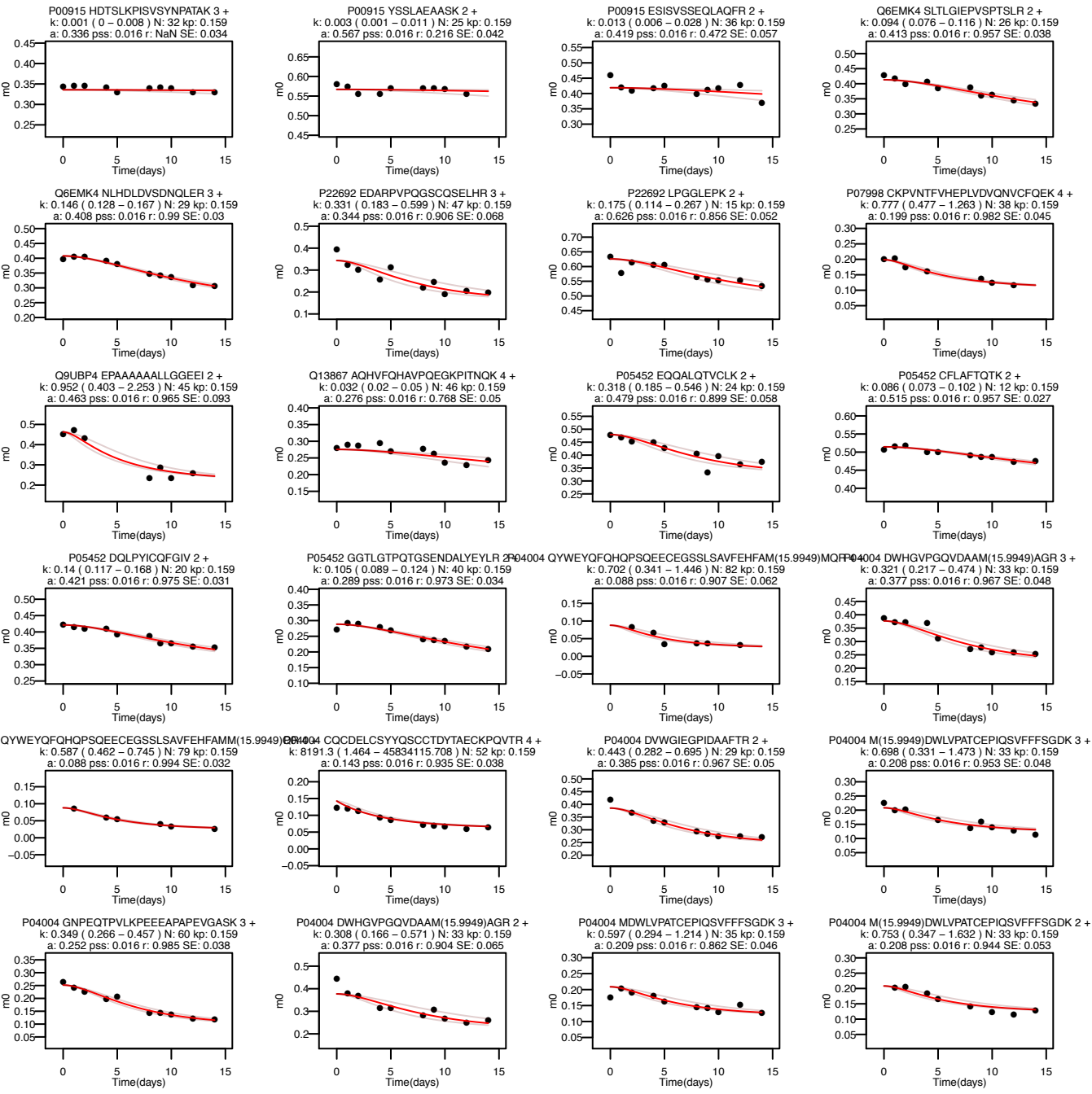


P22352 YVRPGGGFVNFOLFQEK 3 +
k: 0.048 (0.029 - 0.08) N: 28 kp: 0.159
a: 0.308 pss: 0.016 r: 0.702 SE: 0.058

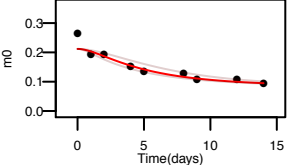


Q9UBR2 NSWGEPWGER 2 +
k: 0.238 (0.12 - 0.469) N: 23 kp: 0.159
a: 0.498 pss: 0.016 r: 0.929 SE: 0.135

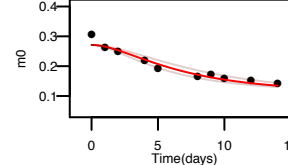




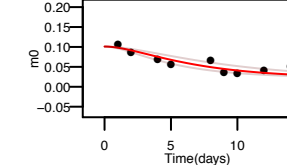
P04004 NISDGFDPDNDVAALPAHSYSYSGR 3 +
k: 0.784 (0.35 - 1.759) N: 57 kp: 0.159
a: 0.212 pss: 0.016 r: 0.931 SE: 0.062



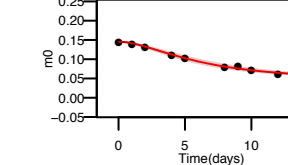
P04004 PETLHPGRPOPPEAEELCSGK 3 #P04004 GNEPQTPVLKPEEEAPAVEVASKGPEGIDSRPETHLPGRPOPPEAEELCSGKPFDAFTDLK 3 +
k: 0.376 (0.248 - 0.571) N: 53 kp: 0.159
a: 0.271 pss: 0.016 r: 0.964 SE: 0.049



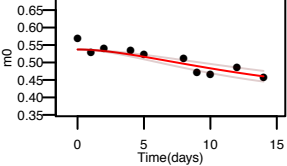
P04004 GNEPQTPVLKPEEEAPAVEVASKGPEGIDSRPETHLPGRPOPPEAEELCSGKPFDAFTDLK 3 +
k: 0.296 (0.175 - 0.502) N: 96 kp: 0.159
a: 0.101 pss: 0.016 r: 0.876 SE: 0.048



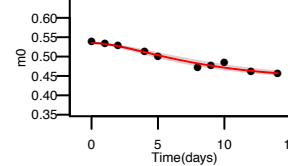
P04004 PETLHPGRPOPPEAEELCSGKPFDAFTDLK 3 +
k: 0.407 (0.319 - 0.521) N: 86 kp: 0.159
a: 0.145 pss: 0.016 r: 0.987 SE: 0.028



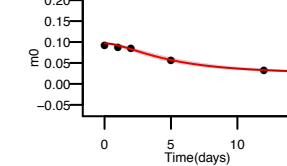
P04004 IYISGMAPR 2 +
k: 0.109 (0.075 - 0.159) N: 18 kp: 0.159
a: 0.537 pss: 0.016 r: 0.894 SE: 0.052



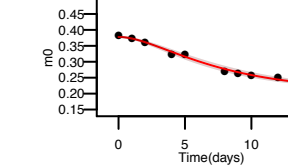
P04004 PFDAFTDLK 2 +
k: 0.345 (0.252 - 0.471) N: 12 kp: 0.159
a: 0.535 pss: 0.016 r: 0.979 SE: 0.031



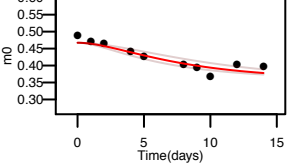
P04004 PEGIDSRPETHLPGRPOPPEAEELCSGKPFDAFTDLK 6 +
k: 0.609 (0.452 - 0.819) N: 83 kp: 0.159
a: 0.097 pss: 0.016 r: 0.993 SE: 0.047



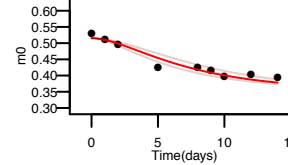
P04004 DWHGVPGVQVDAAMAGR 3 +
k: 0.333 (0.278 - 0.4) N: 37 kp: 0.159
a: 0.378 pss: 0.016 r: 0.993 SE: 0.032



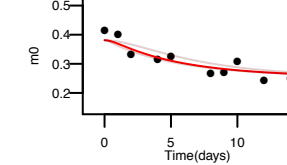
P12259 PYYSDVDIMR 2 +
k: 0.366 (0.204 - 0.659) N: 16 kp: 0.159
a: 0.467 pss: 0.016 r: 0.929 SE: 0.049



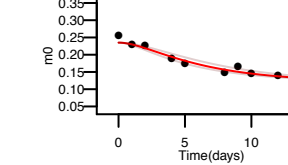
P12259 SEAYNTFSER 2 +
k: 0.409 (0.26 - 0.645) N: 23 kp: 0.159
a: 0.515 pss: 0.016 r: 0.961 SE: 0.053



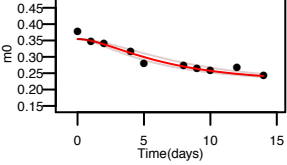
P12259 DIHSGLIGPLLICQK 2 +
k: 1.738 (0.45 - 6.706) N: 25 kp: 0.159
a: 0.381 pss: 0.016 r: 0.912 SE: 0.063



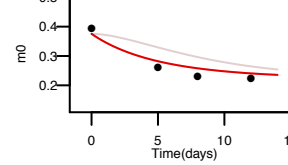
P12259 EKPOSTISGLLGPTLYAEVGDIIK 3 +
k: 0.515 (0.325 - 0.815) N: 42 kp: 0.159
a: 0.235 pss: 0.016 r: 0.968 SE: 0.045



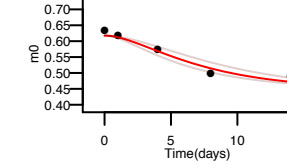
P12259 PGWLLNTEVEGNOR 2 +
k: 0.501 (0.312 - 0.806) N: 16 kp: 0.159
a: 0.354 pss: 0.016 r: 0.964 SE: 0.044



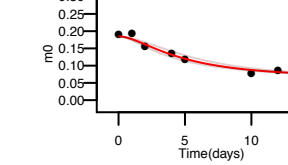
P12259 GEYEEHLGILGPIIR 2 +
k: 32767.3 (0.255 - 4217499808.638) N: 32 kp: 0.159
a: 0.375 pss: 0.016 r: 0.953 SE: 0.204



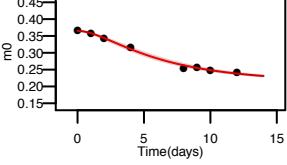
P12259 LAAEFASK 2 +
k: 0.411 (0.243 - 0.696) N: 20 kp: 0.159
a: 0.618 pss: 0.016 r: 0.974 SE: 0.103



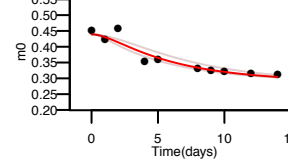
P12259 HLSQDQTSPSGMRPWEDLPDQTGSPSR 4 +
k: 0.769 (0.468 - 1.263) N: 62 kp: 0.159
a: 0.185 pss: 0.016 r: 0.98 SE: 0.053



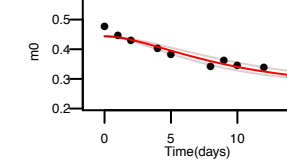
P12259 LSEGASYLDHTTFAEK 3 +
k: 0.571 (0.471 - 0.694) N: 33 kp: 0.159
a: 0.365 pss: 0.016 r: 0.997 SE: 0.032



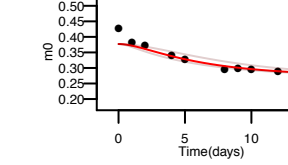
P12259 SOHLDNFSNOIGK 3 +
k: 0.8 (0.396 - 1.615) N: 26 kp: 0.159
a: 0.439 pss: 0.016 r: 0.95 SE: 0.054



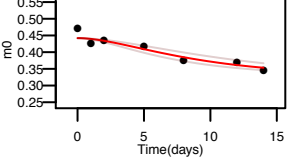
P12259 ADKPSIHPOGIR 3 +
k: 0.241 (0.171 - 0.341) N: 29 kp: 0.159
a: 0.443 pss: 0.016 r: 0.962 SE: 0.049



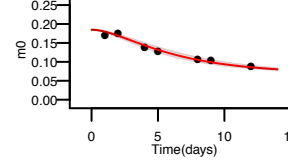
P12259 VMYTYQYEDSFTK 2 +
k: 0.73 (0.297 - 1.793) N: 20 kp: 0.159
a: 0.377 pss: 0.016 r: 0.929 SE: 0.054



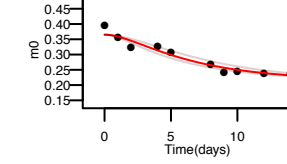
P12259 HEDTLTLFPMR 3 +
k: 0.268 (0.157 - 0.456) N: 18 kp: 0.159
a: 0.442 pss: 0.016 r: 0.942 SE: 0.067



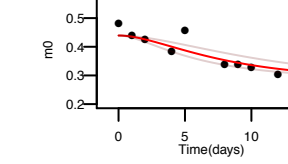
P12259 HLSQDQTSPSGMRPWEDLPDQTGSPSR 3 +
k: 0.43 (0.33 - 0.56) N: 62 kp: 0.159
a: 0.185 pss: 0.016 r: 0.985 SE: 0.042

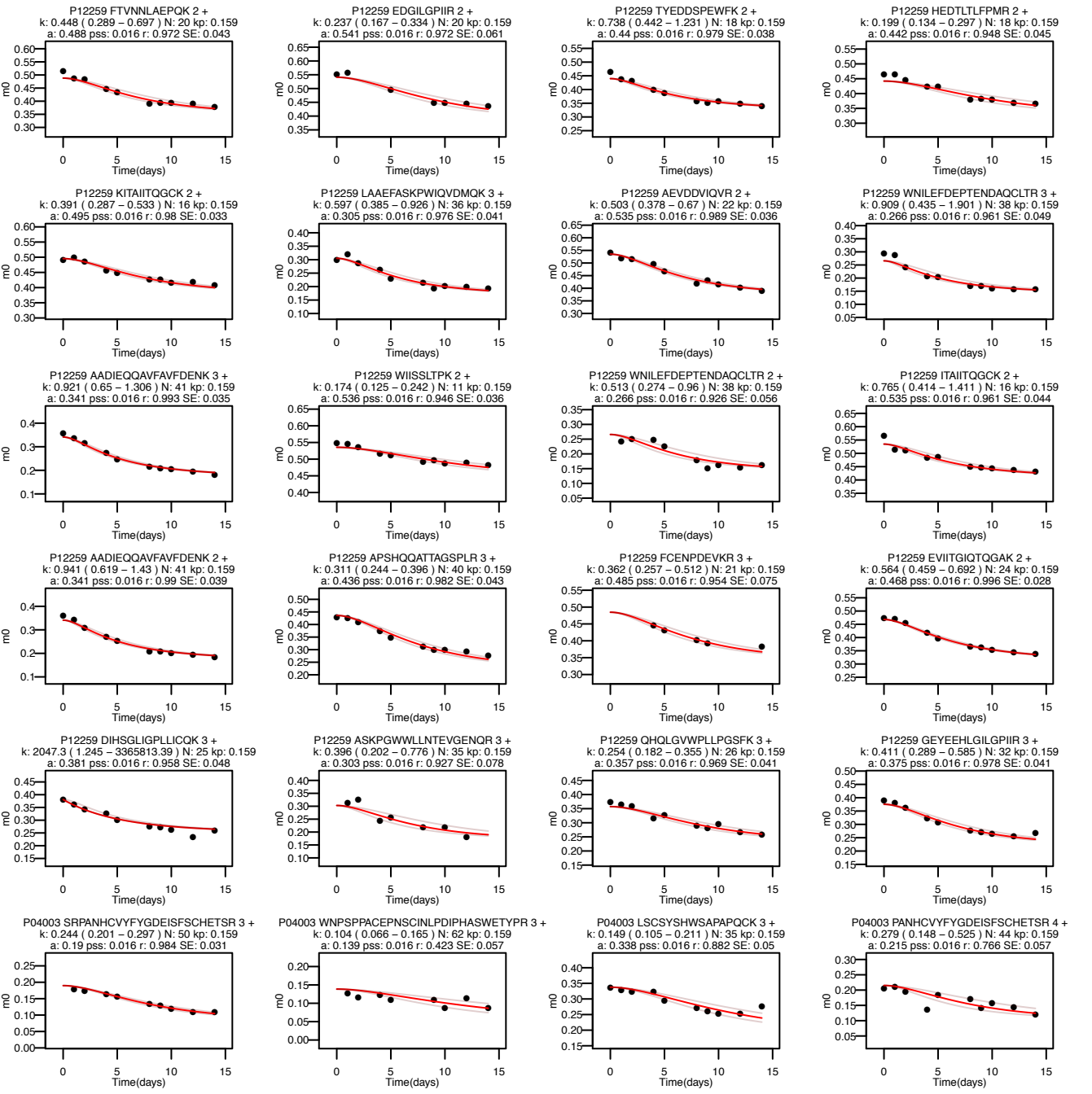


P12259 LSEGASYLDHTTFAEK 2 +
k: 0.515 (0.318 - 0.834) N: 33 kp: 0.159
a: 0.365 pss: 0.016 r: 0.967 SE: 0.048

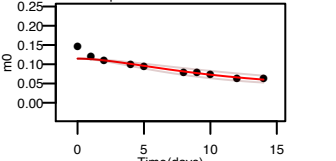


P12259 SOHLDNFSNOIGK 2 +
k: 0.329 (0.162 - 0.668) N: 26 kp: 0.159
a: 0.439 pss: 0.016 r: 0.901 SE: 0.068

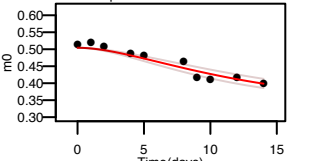




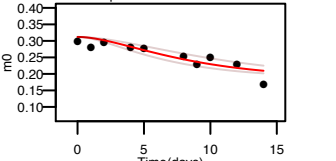
WNPSPPACEPNSINLPDIHAWSETYPRRKT 4 +
k: 0.158 (0.101 - 0.247) N: 66 kp: 0.159
a: 0.115 pss: 0.016 r: 0.912 SE: 0.042



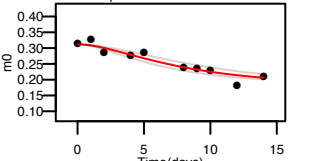
P04003 GSSVHCHADSJK 2 +
k: 0.142 (0.106 - 0.191) N: 24 kp: 0.159
a: 0.504 pss: 0.016 r: 0.954 SE: 0.048



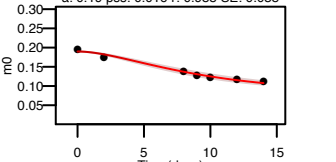
P04003 WTPYQGCEALCCPEPK 3 +
k: 0.273 (0.158 - 0.472) N: 32 kp: 0.159
a: 0.312 pss: 0.016 r: 0.878 SE: 0.055



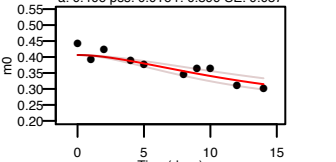
P04003 WTPYQGCEALCCPEPK 2 +
k: 0.324 (0.201 - 0.525) N: 32 kp: 0.159
a: 0.312 pss: 0.016 r: 0.949 SE: 0.049



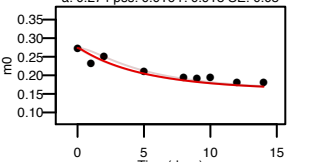
P04003 SRPANHCYVYFGDEISFSCHESTR 5 +
k: 0.211 (0.174 - 0.256) N: 50 kp: 0.159
a: 0.19 pss: 0.016 r: 0.988 SE: 0.038



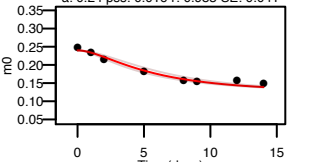
P04003 FSAICQGDGTWSPR 2 +
k: 0.125 (0.083 - 0.187) N: 28 kp: 0.159
a: 0.406 pss: 0.016 r: 0.899 SE: 0.057



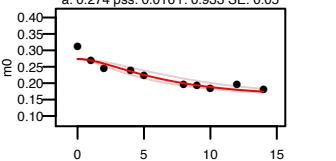
P08709 LHQPVLVDHVPVLPCLPER 4 +
k: 8.8 (1.119 - 69.23) N: 33 kp: 0.159
a: 0.274 pss: 0.016 r: 0.918 SE: 0.05



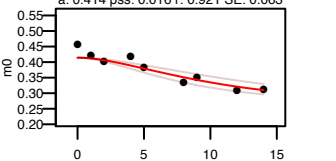
P08709 VAQVIPSTYVPGTTHNDIALLR 3 +
k: 0.679 (0.447 - 1.031) N: 39 kp: 0.159
a: 0.24 pss: 0.016 r: 0.983 SE: 0.041



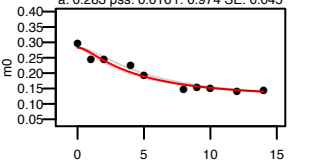
P08709 LHQPVLVDHVPVLPCLPER 3 +
k: 0.484 (0.258 - 0.905) N: 33 kp: 0.159
a: 0.274 pss: 0.016 r: 0.933 SE: 0.05



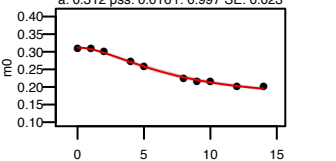
P08709 GATALEMLVNLNVR 2 +
k: 0.192 (0.117 - 0.315) N: 26 kp: 0.159
a: 0.414 pss: 0.016 r: 0.921 SE: 0.063



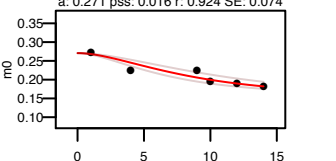
P08709 NLIAVLGEHDLSEHDGDEQSR 3 +
k: 1.8 (0.863 - 3.756) N: 49 kp: 0.159
a: 0.283 pss: 0.016 r: 0.974 SE: 0.045



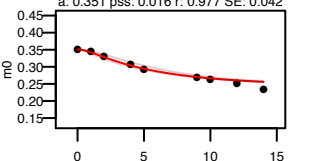
P13671 ENPAVIDFELAPIVDLVR 3 +
k: 0.679 (0.447 - 1.031) N: 39 kp: 0.159
a: 0.312 pss: 0.016 r: 0.997 SE: 0.023



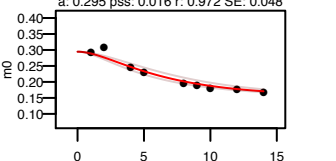
P13671 TECIKPVVQEVLTITPFQR 3 +
k: 0.268 (0.163 - 0.441) N: 33 kp: 0.159
a: 0.271 pss: 0.016 r: 0.924 SE: 0.074



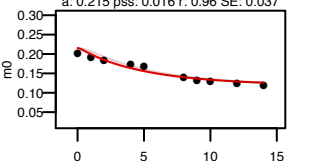
P13671 KESCGYDTCYDWEK 3 +
k: 1.378 (0.631 - 3.011) N: 22 kp: 0.159
a: 0.351 pss: 0.016 r: 0.977 SE: 0.042



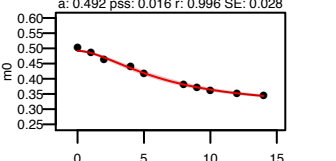
P13671 VPANLNVGFVQTAEDDLK 2 +
k: 0.476 (0.308 - 0.736) N: 40 kp: 0.159
a: 0.295 pss: 0.016 r: 0.972 SE: 0.048



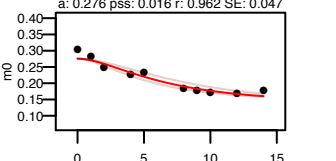
P13671 CPINCLLGDGFGPWSDCDPCIEK 3 +
k: 5.8 (1.347 - 24.98) N: 37 kp: 0.159
a: 0.215 pss: 0.016 r: 0.96 SE: 0.037



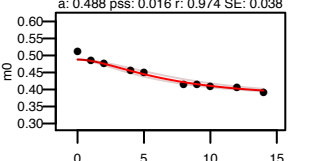
P13671 SEYGAALAWEK 2 +
k: 0.53 (0.444 - 0.634) N: 26 kp: 0.159
a: 0.492 pss: 0.016 r: 0.996 SE: 0.028



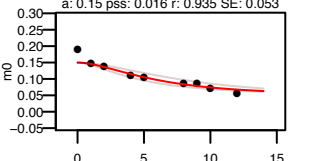
P13671 CLNNOQLHFLHIGSCQDGR 4 +
k: 0.443 (0.273 - 0.717) N: 40 kp: 0.159
a: 0.276 pss: 0.016 r: 0.962 SE: 0.047



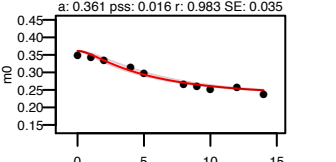
P13671 TFSEWLESVK 2 +
k: 0.517 (0.323 - 0.827) N: 15 kp: 0.159
a: 0.488 pss: 0.016 r: 0.974 SE: 0.038



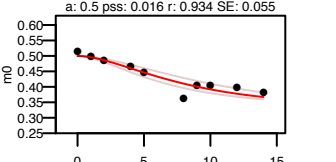
P13671 DLTLSGHNNQQGSFSSQGGSSFSVPFYSSK 4
k: 0.441 (0.235 - 0.825) N: 64 kp: 0.159
a: 0.15 pss: 0.016 r: 0.935 SE: 0.053



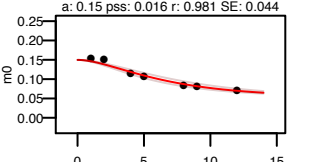
P13671 YYQENFCEQICSK 2 +
k: 1.394 (0.766 - 2.535) N: 26 kp: 0.159
a: 0.361 pss: 0.016 r: 0.983 SE: 0.035



P13671 SENINHNSAFK 3 +
k: 0.312 (0.193 - 0.504) N: 24 kp: 0.159
a: 0.5 pss: 0.016 r: 0.934 SE: 0.055



P13671 DLTLSGHNNQQGSFSSQGGSSFSVPFYSSK 3 +
k: 0.361 (0.261 - 0.499) N: 64 kp: 0.159
a: 0.15 pss: 0.016 r: 0.981 SE: 0.044



P13671 ESCGYDTCYDWEK 2 +
k: 4095.3 (1.265 - 1325432.729) N: 21 kp: 0.159
a: 0.379 pss: 0.016 r: 0.953 SE: 0.043

